

Max-Delbrück-Centrum für Molekulare Medizin
in der Helmholtz-Gemeinschaft

DISSERTATION

Gehirnhistamin wirkt auf Mikroglia hauptsächlich über
Astrozyten
Brain histamine acts on microglia mainly via astrocytes

zur Erlangung des akademischen Grades
Doctor medicinae (Dr. med.)

vorgelegt der Medizinischen Fakultät
Charité – Universitätsmedizin Berlin

von

Herrn Pengfei Xia

aus Jiangsu, China

Datum der Promotion: 04.03.2022

Table of Contents

List of abbreviations	3
1. Abstract.....	4
1.1 English.....	4
1.2 Deutsch	5
2. Manteltext	6
2.1 State of the art - research	6
2.2 Methodology	9
2.3 Essential new results	12
2.4 Futher scientific questions	17
2.5 References:	20
3. Statutory Declaration	23
4. Declaration of your own contribution to the publications	24
5. Excerpt of Journal Summary List “Neurosciences”	25
6. Publication	27
7. Curriculum Vitae	55
8. Publication List.....	56
9. Acknowledgements.....	57

List of abbreviations

Hrh	Histamine receptors
HDC	Histidine decarboxylase
TMN	Tuberomamillary nucleus
MACS	Magnetic-activated cell sorting
ACSF	Artificial cerebrospinal fluid
CNS	Central nervous system
PBS	Phosphate-buffered solution
PFA	Paraformaldehyde
Ca ²⁺	Calcium
InsP ₃	Inositol 1,4,5-triphosphate
PLC	Phospholipase C
GPCR	G protein-coupled receptors
CRAC	Ca ²⁺ release-activated channels
SERCA	Sarco(endo)plasmic reticulum Ca ²⁺ -ATPases
PMCA	Plasmalemmal Ca ²⁺ -ATPase
NCX	Na ⁺ /Ca ²⁺ exchanger
ER	Endoplasmic reticulum
P2X	Ionotropic purinergic receptor
P2Y	Metabotropic purinergic receptor
LPS	Lipopolysaccharide

I. Abstract

1.1 (English)

Microglia, as the resident immune cells in the central nervous system, react to the micro-environment changes and maintain the hemostasis of the brain. It has been illustrated that multiple neurotransmitters including histamine induce diversity effects on the properties of microglia under normal physiological and pathophysiological conditions. As a monoaminergic neurotransmitter, Histamine is produced and further released by neuronal cells mostly located in tuberomammillary nucleus of hypothalamus. Despite the fact that the function of histamine in modulating neural fire patterns, it is also believed that histamine is capable to regulate the function of glial cells. In the present study, we demonstrate that primary cultured microglia respond to histamine with intracellular Ca^{2+} increases, which depend on microglial *Hrh2* receptors. Moreover, these results were validated by *Hrh2* specific agonists and inhibitors together with a comprehensive metadata analysis of microglial transcriptome sequencing. Nevertheless, in acute cortical and thalamic brain slices from a newly established, microglia-specific Ca^{2+} indicator mouse line, microglia respond to histamine mainly in a *Hrh1*-dependent manner, while *Hrh2*-mediated responses were less detectable. The *Hrh1* response was also shown to be sensitive to inhibitors of *P2ry12* purinergic receptors. Base on the fact that *Hrh1* is mostly expressed by astrocytes in the brain, it is assumed that the *Hrh1* response in microglia is mediated by the astrocyte releasing ATP, which followed by activation of *P2ry12* receptors in microglia. In addition, histamine enhanced microglial phagocytosis activity via *Hrh1*- and *P2ry12*-mediated signaling. Taken together, the present study demonstrate that histamine has an indirect effect on the Ca^{2+} level changes of the microglia and their phagocytic activity via astrocytic histamine receptors as well as purinergic signaling pathway.

1.2 (Deutsch)

Mikroglia sind die angeborenen Immunzellen und professionellen Phagozyten des Zentralnervensystems, und es ist bereits bekannt, dass Histamin mehrere Auswirkungen auf die Funktionen von Mikroglia unter physiologischen und pathophysiologischen Konditionen haben kann. Histamin ist ein monoaminerges Neurotransmitter, der von Neuronen aus dem tuberomammillären Kern in allen Hirnregionen freigesetzt wird. Neben der Modulation neuronaler Feuermuster wird angenommen, dass der Histaminspiegel im Gehirn auch die Funktion von Gliazellen moduliert. In der vorliegenden Arbeit wird gezeigt, dass isolierte Mikrogliazellen auf Histamin mit intrazellulären Ca^{2+} -Erhöhungen reagieren, was auf mikrogliale *Hrh2*-Rezeptoren zurückzuführen ist, wie ich durch spezifische Agonisten und Antagonisten sowie eine Metadatenanalyse von Mikroglia-Transkriptomen bestätigen konnte. In akuten kortikalen und thalamischen Hirnschnittpräparaten aus einer neuen, mikroglia-spezifischen Ca^{2+} -Indikator-Mauslinie reagierten Mikroglia überraschenderweise hauptsächlich in einer *Hrh1*-abhängigen Weise auf Histamin, während *Hrh2*-vermittelte Antworten nur in geringem Ausmaß nachweisbar waren. Interessanterweise stellte sich die *Hrh1*-Antwort als empfindlich gegenüber Inhibitoren purinerges *P2ry12*-Rezeptoren heraus. Da *Hrh1* im Gehirn vorwiegend von Astrozyten exprimiert wird, liegt es nahe, dass die *Hrh1*-Antwort in Mikroglia durch eine ATP-Freisetzung aus Astrozyten und die anschließende Aktivierung von *P2ry12*-Rezeptoren in Mikroglia vermittelt wird. Histamin stimulierte auch die mikrogliale phagozytische Aktivität über *Hrh1*- und *P2ry12*-vermittelte Signale. Zusammengefasst liefert die vorliegende Arbeit Hinweise darauf, dass Histamin im Gehirn über astrozytäre Histaminrezeptoren und purinerge Signalwege indirekt auf die Ca^{2+} -Level der Mikroglia und deren phagozytische Aktivität wirkt.

2. Manteltext

2.1 State of the art – research

Microglia are the resident immune cells in the brain and they are classified as central nervous system (CNS) macrophages in terms of morphological and physiological functions (Hanisch and Kettenmann, 2007). In the healthy brain, microglia display a ramified phenotype and constantly monitor changes in the surrounding environment (Nimmerjahn *et al.*, 2005). However, in response to pathological conditions such as inflammation or ischemia, microglia transform from a ramified, surveilling phenotype to an activated state which is characterized by morphological transformations as well as changes in functional behavior including phagocytosis, the release of a variety of substances, migration, and proliferation (Hanisch and Kettenmann, 2007, Kettenmann *et al.*, 2011). Microglia play an important role in supporting, nourishing, protecting and repairing the CNS in development and under physiological conditions, and they are involved in different brain diseases (Wolf *et al.*, 2017). Activation of microglia upon changes in brain homeostasis is a complex process involving multiple stimuli and multiple membrane receptors. Microglia also express receptors for neurotransmitters, such as GABA, acetylcholine and histamine (Pocock and Kettenmann, 2007, Kettenmann *et al.*, 2011, Pannell *et al.*, 2016). These receptors not only modulate microglial physiology but also suggest their potential involvement in regulation of neurogenesis, synaptic development and synaptic plasticity, and have a regulatory effect on chronic brain inflammation, neurodegenerative diseases and mental disorders (Kettenmann *et al.*, 2011).

Histamine is a biologically active amine substance. In the peripheral system, it can regulate many physiological processes such as allergic reactions, gastric acid secretion, and itching (Thangam *et al.*, 2018). In the central nervous system, histamine is synthesized by the neurons which expressing l-histidine decarboxylase (HDC). These neurons are located in the tuberomamillary nucleus (TMN) and send axonal projections towards essentially all brain regions (Haas and Panula, 2003, Panula and Nuutinen, 2013). Histamine neurons are pacemakers and exhibit regular spontaneous discharge patterns at low frequency, this is related to the sleep/wake rhythm with upregulation of histamine release during wakefulness (Vitrac and Benoit-Marand, 2017). Abnormal brain histamine release is increasingly recognized as a potential cause of brain pathology such as Alzheimer's disease, Huntington's disease, Parkinson's disease, narcolepsy and drug addiction (Panula and Nuutinen, 2013). The effect of histamine is mediated by the downstream signals of the four mammalian histamine receptor subtypes (*Hrh1-Hrh4*), the four subtypes are $G\alpha_q$ (*Hrh1*), $G\alpha_s$ (*Hrh2*) or $G\alpha_i$ (*Hrh3* and *Hrh4*) protein-coupled receptors.

Recent transcriptomic and proteomic studies suggest that *Hrh1-Hrh3* are clearly expressed in the central nervous system, whereas *Hrh4* expression is not sure (Juric *et al.*, 2016, Zhang *et al.*, 2014). The main subtype in the brain is *Hrh3* which is mainly expressed by neurons and which regulates the release of various neurotransmitters such as GABA and acetylcholine from neurons (Passani *et al.*, 2000), *Hrh1* and *Hrh2* are also expressed at low levels in neurons. However, previous gene expression researches and functional studies indicate that these isoforms are more likely regulators of glial function (Zhang *et al.*, 2014). In particular, *Hrh1* is the most abundant subtype in astrocytes (Jung *et al.*, 2000), adjust various physiological and pathological activities of astrocytes according to changes in brain histamine levels, including energy metabolism, neurotransmitter clearance, neurotrophic activity and immune response (Juric *et al.*, 2016).

Calcium (Ca^{2+}) is an ubiquitous intracellular messenger which is involved in a wide range of microglia functions. Many features of microglia have previously been shown to be related to intracellular Ca^{2+} pathways. One major Ca^{2+} signaling cascade in microglial cells is via Inositol 1,4,5-triphosphate (InsP_3)-gated Ca^{2+} release from InsP_3 receptors located on the endoplasmic reticulum (ER). InsP_3 is generated by phospholipase C (PLC) which activity is controlled by G protein-coupled receptors (GPCRs). In addition, microglia express a wide selection of membrane-bound Ca^{2+} channels, allowing Ca^{2+} to enter the cytosol directly from the extracellular space. The summary of the Ca^{2+} signaling in microglia is shown in Figure 1 (Kettenmann *et al.*, 2011).

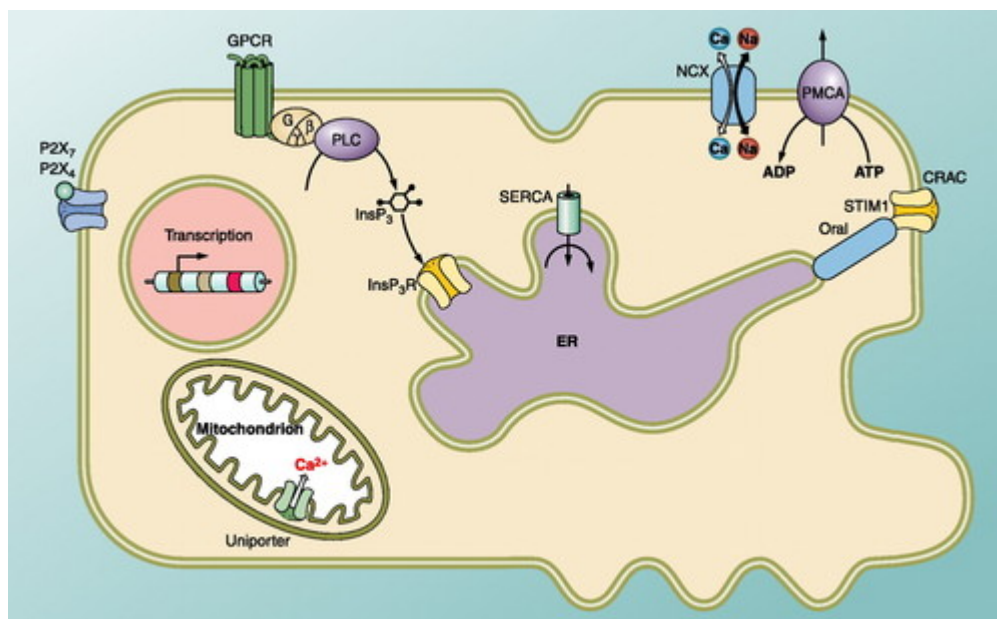


Figure 1. Calcium signaling in microglia. The main calcium signaling cascades in microglial cells are represented by 1) InsP_3 -induced Ca^{2+} release from the ER. The InsP_3 is

generated by PLC coupled with multiple G protein-coupled receptors (GPCR). Depletion of the ER Ca^{2+} store activates the store-operated channels (CRAC) which are likely to be formed through interactions between STIM1/Orai proteins. 2) Ca^{2+} influx through P2X_7 and/or P2X_4 receptors constitutively expressed in microglia. The extrusion of Ca^{2+} from the cytosol is accomplished by 1) Ca^{2+} uptake into the ER via sarco(endo)plasmic reticulum Ca^{2+} -ATPases (SERCA); 2) Ca^{2+} accumulation in mitochondria through Ca^{2+} -selective uniporters, and 3) Ca^{2+} extrusion to the extracellular space by plasmalemmal Ca^{2+} -ATPase (PMCA) and $\text{Na}^+/\text{Ca}^{2+}$ exchangers (NCX). Figure adapted from *Kettenmann et al., 2011*.

Microglial intracellular Ca^{2+} can be regulated by various GPCR including those for neurotransmitters (Inoue, 2002, Moller, 2002, Farber, Kettenmann, 2006 and Kettenmann 2011). Increases in intracellular Ca^{2+} are closely related to microglial functions including the release of pro-inflammatory, anti-inflammatory and nutrient factors (Inoue, 2002).

The first evidence of a microglial response to histamine receptor activation was demonstrated via Ca^{2+} imaging on primary cultured rat microglia (Bader *et al.*, 1994) and later confirmed on primary cultured and freshly isolated mouse microglia (Pannell *et al.*, 2014). More recent studies report also the involvement of histamine on microglial functions like phagocytosis. However, there is still a quite diverse and partially controversial picture of histamine action, microglial *Hrh* expression and its functional impact (Rocha *et al.*, 2016, Iida *et al.*, 2015, Apolloni *et al.*, 2017). However, all these data were mainly obtained from *in vitro* experiments. Currently, little is known about the calcium signaling of microglia *in situ* or *in vivo*.

The present study aims to use a novel microglia-specific Ca^{2+} indicator mouse model to investigate microglial Ca^{2+} elevations upon histamine and *Hrh*-specific agonists in the different brain regions. We provide evidence for functional *Hrh2*, but not *Hrh1*, *Hrh3* or *Hrh4* expression on microglia and identified that astrocytes communicate with microglia via purinergic signaling upon *Hrh1* stimulation.

2.2 Methodology

In the current study, to perform live cell Ca^{2+} imaging on microglia *in vitro*, I acutely isolated microglia using magnetic-activated cell sorting (MACS) to prepare freshly isolated microglia as described previously (Nikodemova and Watters, 2012). Briefly, to obtain the isolated microglia, adult C57BL/6 mice were perfused using an ice-cold PBS solution under deep anesthesia, after decapitation, the brains were extracted and placed on ice with HBSS after removal of the cerebellum and the olfactory bulbs. Only the cortex was dissected and homogenized into Miltenyi Biotec adult brain Dissociation Kit (Trypsin), and then dissociated in the gentleMACS Octo Dissociator for 30 min. After the resuspended pellets were passed through a MACS smart strainer (70 μm), the single cell suspension was resuspended in ice-cold debris removal solution (Miltenyi Biotec). a layer of PBS was applied on top and centrifuged at 3000g, 4°C full brake and full acceleration. Labeled CD11b-positive cells were collected through large-sized MACS columns (Miltenyi Biotec, Bergisch Gladbach, Germany). Then acutely isolated microglial cells were plated on glass coverslips. After 2h, adhered microglia were incubated for 40 min with 5 μM Fluo-4/AM (Invitrogen, Carlsbad, CA) in standard extracellular solution (150 mM NaCl, 5.4 mM KCl, 0.98 mM MgCl_2 , 1.97 mM CaCl_2 , 10 mM HEPES and 10 mM glucose; pH 7.4) at room temperature.

For *in situ* recordings, acute cortical brain slices from adult male and female C57BL/6, Csf1R-2A-GCaMP6m or Csf1R-2A-mCherry-2A-GCaMP6m mice (P40 - P90) were prepared as previously described (Boucsein *et al.*, 2003). Briefly, adult mice were sacrificed by cervical dislocation. the brains were extracted directly and immediately removed the cerebellum and the olfactory bulbs, then transferred to mount on a metal disc with ice-cold slicing solutions (230 mM sucrose, 26 mM NaHCO_3 , 2.5 mM KCl, 1.25 mM NaH_2PO_4 , 10 mM MgSO_4 , 0.5 mM CaCl_2 , 10 mM D-glucose; pH 7.4; saturated with carbogen: 95% O_2 , 5% CO_2). Coronal sections with the thickness of either 140 μm for phagocytosis assay or 250 μm for Ca^{2+} imaging were cut with a vibratome (Microm HM 650V, Thermo Fisher Scientific, Massachusetts, U.S.A.). Slices containing the regions of interest (cortex, corpus callosum, hippocampus, striatum and thalamus) were obtained. Acute brain slices from Csf1R-2A-GCaMP6m mice were maintained in carbogenized artificial cerebrospinal fluid (ACSF) at RT, while slices (250 μm) from C57/Bl6 mice were generated and loaded with 10 μM Fluo4/AM for 1h at 37°C to stain astrocytes. To demonstrate the fluo4-labelled slice preparations in which the Ca^{2+} indicator dye is exclusively taken up by GFAP+ cells, we have included acute brain slices from GFAP-RFP transgenic mice were labeled with Fluo4-AM.

Coverslips or brain slices were transferred into a recording chamber constantly perfused with standard extracellular solution (isolated microglia) or carbogenized ACSF (brain slices). In each slice, I recorded a specific area

using Ca²⁺ imaging, including cortex, corpus callosum, hippocampus, striatum and thalamus. Each brain slice/coverlip was first examined using a 5X objective and bright field illumination. For Ca²⁺ recordings, I used a 20X objective (Carl Zeiss Microscopy GmbH, Jena, Germany), a Zyla 5.5 camera (Oxford Instruments, Belfast, UK), a light-emitting diode illuminator (pE-4000, CoolLED, Andover, UK) and a standard EGFP filter set. An EPC9 amplifier (HEKA, Lamprecht, Germany) and TIDA 5.25 software (Heka) were used to trigger fluorescence excitation and image acquisition. During Ca²⁺ recording experiments, pictures were taken at a frequency of 1 frame per second and an exposure time of 100 ms. After the substance application, the slice were washed out for 4-5 minutes with ACSF, followed by the application of ATP (1 mM) for 60 s as positive control. Calcium imaging movies were analyzed using a home-made algorithm in Igor Pro 6.37 (WaveMetrics, Lake Oswego, USA). For analysis, we selected the cell somata as ROIs that were visible in the presence of ATP at the end of each experiment, and determined the mean relative fluorescent intensity of each ROI and frame to show changes in Ca²⁺ levels for each cell. Therefore, only microglia or astrocytes with ATP reactions are included in subsequent analysis. Intracellular Ca²⁺ elevations were counted as “responsive” upon application of a substance when microglial Ca²⁺ response amplitudes exceeded three times the SD or astrocytes Ca²⁺ response amplitudes exceeded five times the SD of the baseline. We calculate the response of each slice on average to get one “n” for the subsequent statistic. For the analysis of amplitudes and kinetics of microglial Ca²⁺ responses, we used all “responding” events and excluded non-responders.

To study the effect of brain histamine on microglia at a more functional level, we tested if and how microglia phagocytosis is modulated by histamine. Phagocytosis assay in acute cortical or thalamic brain slices was conducted as previously described (Wendt *et al.*, 2017). After the generation of 140 µm thick coronal or thalamic slices from C57/Bl6 mice, slices were incubated in ACSF constantly gassed with carbogen (95% O₂/ 5% CO₂) for 2 hours at RT, and subsequently incubated at 37°C for 1 h with latex beads (4.5 µm diameter, Polysciences Europe GmbH) and histamine or isoform-specific agonists and antagonists, then washed intensively with 0.1 M PBS (3 x 20 min) and subsequently fixed with 4% paraformaldehyde (PFA) for 1 h. After washing with phosphate-buffered solution (PBS), slices were incubated in a permeabilisation buffer (2% Triton X-100, 2% bovine serum albumin, 10% normal donkey serum) in 0.1 M PBS (pH 7.4) for 4 h, and then overnight with the goat anti-Iba1 antibody (1:600; clone 5076 abcam) in dilution buffer (1:10 of permeabilisation buffer in 0.1 M PBS) at 4°C. On the next day, the slices were incubated with the secondary antibody donkey anti goat Alexa Fluor 647 (1:250; Dianova) for 2 hours. Finally, after washing, the slices were mounted with Aqua Polymount mounting medium on glass slides.

Microglia volumes and bead numbers were calculated using Imaris 6.3.1 (Bitplane, Zürich, Switzerland). The Iba1-positive volumes z-stack images from confocal microscopy (Leica TCS SPE; 20× oil-immersion objective) were 3D-rendered by application of Imaris-internal threshold value of 40 AU, and by a background subtraction (Imaris-internal parameters: 1-3 times, ~90 μm each), Beads were detected as spots and counted automatically (“Split into surface object” plugin), All beads having their center located within a given rendered Iba1 volume were considered to be phagocytosed by microglia. The phagocytic index was calculated by the following equation:

$$\text{Phagocytic index} = \frac{n_{\text{PM}} * 10^4}{V_{\text{Iba1}}}$$

n_{PM} is the total number of phagocytosed microspheres and V_{Iba1} is the Imaris-rendered volume of Iba1 fluorescence in μm³.

The cell type-specific expression of *Hrh* isoforms and the brain region-specific microglial RNAseq dataset at different ages were obtained from the website www.brainrnaseq.org and GEO site GSE62420. For *Hrh* and *P2ry12* expression in single microglia, we utilized the online tools on <https://tabulamuris.ds.czbiohub.org/> and exported the resulting plots.

All data are given as median ± 25%/75% percentile or mean ± SEM. Statistical significance was tested by the Kruskal-Wallis followed by a Dunn’s multiple comparison test using Graphpad Prism 7.04. Statistical significance levels are given by n.s.: p>0.05; *: p < 0.05; **: p < 0.01; ***: p < 0.001.

A detailed description of all methods applied for this study can be found in the materials and methods section of Xia *et al.* (2021).

2.3 Essential new results

Xia *et al* demonstrated for the first time that histamine acts indirectly on microglial Ca²⁺ levels and phagocytic activity via astrocyte histamine receptor-controlled purinergic signaling.

Previous studies from our group revealed that primary cultured microglia and freshly isolated microglia functionally express histamine receptors. First, we investigated freshly isolated microglia, and the percentage of microglia responding to histamine ($5.88 \pm 2.98/8.00\%$; $n = 502$ cells; 15 coverslips; 4 mice) was significantly higher than spontaneous Ca²⁺ elevations ($p = 0.0021$). Additionally, there are four known histamine receptor isoforms (*Hrh1-4*) in the mammalian genome (Passani *et al.*, 2000). We used *Hrh* isoform-specific agonists to identify the receptor isoform responsible for microglial histamine responses. Isolated microglia only responded to *Hrh2*-specific agonist amthamine ($4.17 \pm 2.38/11.83\%$; $n = 1345$ cells; 25 coverslips; 7 mice), there was also no response to *Hrh1*, *Hrh3* and *Hrh4* activation (Figure 2A, B from Xia *et al.*, 2021).

Microglia Ca²⁺ recordings *in situ* were performed by using a novel transgenic Ca²⁺ indicator mouse model (Csf1R-2A-GCaMP6m), histamine and *Hrh* isoform-specific agonists. Our data indicate the proportion of microglia response to histamine in cortex ($12.1 \pm 5.3/20.0\%$; $n = 747$ cells; 45 recordings; 11 mice) and thalamus ($25.0 \pm 11.9/45.8\%$; $n = 253$ cells, 37 recordings, 12 mice). Next we used *Hrh1* and *Hrh2* isoform-specific agonists to identify the receptor isoform responsible for microglial histamine responses. Cortical microglial Ca²⁺ elevations upon histamine *in situ* were evoked mainly through *Hrh1* as demonstrated by using *Hrh1* isoform-specific agonists ($13.4 \pm 0.0/25.6\%$; $n = 184$ cells, 24 recordings, 4 mice) and *Hrh2* isoform-specific agonists ($4.6 \pm 0.0/17.1\%$; $n = 184$ cells, 24 recordings, 4 mice) (Figure 2C, D from Xia *et al.*, 2021). Like in cortex, there was also a significant portion of microglia responding to the *Hrh1* ($18.2 \pm 9.6/34.1\%$; $n = 396$ cells, 43 recordings, 6 mice) and *Hrh2* ($13.4 \pm 8.3/19.6\%$; $n = 354$ cells, 34 recordings, 6 mice) in thalamus. Taken together, both in cortex and thalamus, *Hrh1* resulted being more predominantly involved on microglial histamine responses. These findings were in contrast with the results from isolated microglia where the *Hrh2* was observed as the only microglia-intrinsic histamine receptor. It suggests that the microglia *Hrh1*-mediated response could be indirect and mediated by another cell type. A meta-analysis of several data sets revealed that indeed *Hrh2* is the predominant isoform in microglia whereas *Hrh1* is mainly expressed by astrocytes (Zhang *et al.*, 2014). Astrocytic cells could be then a potential source of signaling substances that are released in a histamine (*Hrh1*)-dependent fashion and then sensed by microglia.

Astrocytic Ca²⁺ level changes in response to histamine and *Hrh* isoform-

specific agonists were investigated *in situ* by loading brain slices from C57/Bl6 mice with the Ca^{2+} indicator Fluo4/AM which is taken up mainly by astrocytes. To demonstrate this Fluo4/AM labeling specificity, the acute brain slices from GFAP-RFP transgenic mice were labelled with Fluo4-AM displayed that $88.6 \pm 6.6\%$ of the RFP+ cells were labelled with Fluo4, and $95.9 \pm 3.9\%$ of the fluo4-labelled cells were positive RFP+. We therefore conclude that most of the Fluo4-labelled cells in our slices are astrocytes.

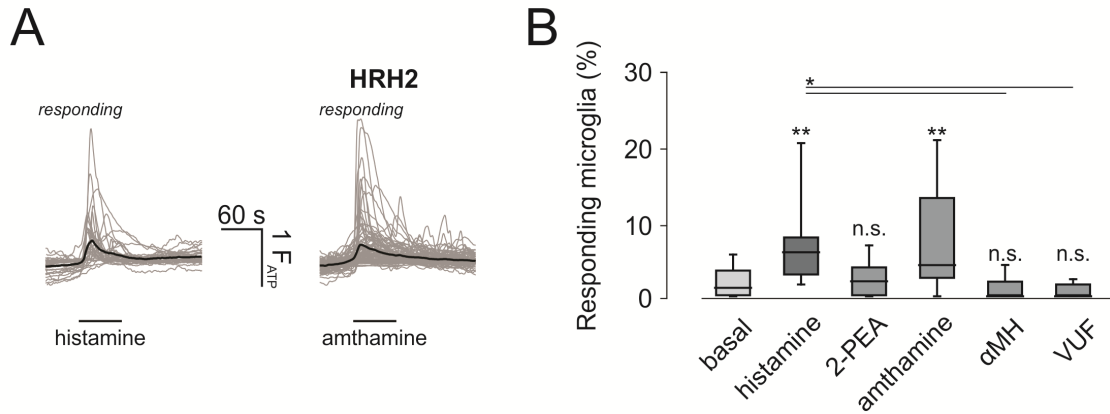
The result of cortical astrocytic Ca^{2+} level changes in response to histamine was $76.5 \pm 52.5/87.9\%$ (n = 143 cells; 11 recordings, 3 mice). *Hrh* isoform-specific agonists *in situ* suggested that *Hrh1* is the dominant histamine receptor isoform in cortical astrocytes ($80.0 \pm 66.7/88.9\%$; n = 124 cells, 10 recordings, 3 mice). The astrocytic response rate upon the *Hrh2* agonist amthamine was only $6.5 \pm 0.0/20.5\%$ (n = 129 cells; 11 recordings, 3 mice). Like in cortex, there was a significant portion of astrocytes in thalamus responding through *Hrh1* ($60.0 \pm 39.7/79.7\%$; n = 133 cells, 13 recordings, 4 mice), but not through *Hrh2* ($0.0 \pm 0.0/0.0\%$; n = 147 cells, 16 recordings, 4 mice). Taken together, astrocytes express functional Histamine receptors in cortex and thalamus, *Hrh1* is the major histamine receptor isoform expressed intrinsically in astrocyte cells and mediates Ca^{2+} responses upon histamine stimulation. Thus, astrocytes could be potential sources of a *Hrh1*-dependent secondary signaling towards microglial receptors.

Previous studies have detected functional purinergic in microglia, and ATP-mediated intercellular communication is a mechanism by which astrocytes communicate and modulate the activity of microglia, thus suggesting that astrocytic Ca^{2+} elevations can be followed by ATP release may act in astrocyte-to-microglia communication which induced subsequent microglial Ca^{2+} responses (Schipke *et al.*, 2002, Verderio and Matteoli, 2001). Our above results indicate that astrocytes but not microglia respond to *Hrh1* isoform-specific agonist *in situ*. In an attempt to test for the hypothesis that the histamine-evoked Ca^{2+} elevations in microglia were a consequence of *Hrh1* stimulation in astrocytes and ATP release, we tested the involvement of *P2ry12* which has been identified as the predominant metabotropic purinergic receptor in microglia and uniquely expressed by microglia in the brain. The blockade of *P2ry12* by AR-C69931 (*P2ry12* antagonist) significantly reduced the cortical microglia responses to histamine to levels indistinguishable from baseline activity ($2.70 \pm 0/3,72\%$; n = 590 cells, 23 recordings, 4 mice, p = 0.0012, Figure2E, F from Xia *et al.*, 2021). Histamine responses were also reduced by the presence of AR-C69931 in thalamic microglia ($12.0 \pm 4.6/16.9\%$; n = 393 cells, 20 slices and 4 mice) which was reduced compared to the only histamine application ($25.0 \pm 11.9/45.8\%$). These data suggest that ATP is the messenger that causes cortical microglial Ca^{2+} responses upon histamine application and the purinergic signaling is involved in intercellular signaling between astrocytes and microglial cells.

Furthermore, to study the effect of brain histamine on microglia phagocytosis, we incubated the acute brain slice from adult C57BL/6J mice (P40-P90) for 60 min with latex beads, and subsequent staining for microglia with goat anti-Iba1. Confocal imaging and 3D reconstruction were used to count the number of beads incorporated into a 3D-rendered Iba1-labeled (microglia) volume. Our data demonstrate that histamine significantly enhanced microglial phagocytosis ($2.87 \pm 2.14/3.87$; $n = 90$ VF) as compared to baseline activity ($1.65 \pm 0.93/2.47$; $n = 54$ VF, $p < 0.0001$) in cortex. Comparing the number of microglial cells incorporating with beads, our data revealed that histamine increased the number of phagocytosing cells (1 beads: 12.3 ± 0.7 and 6.7 ± 0.6 microglia/VF; 2 beads: 1.6 ± 0.3 and 4.4 ± 0.4 microglia/VF; 3 beads: 0.5 ± 0.1 and 1.6 ± 0.2 microglia/VF; 4 beads: 0.1 ± 0.1 and 0.7 ± 0.1 microglia/VF, respectively, $p < 0.0001$). Interestingly, the histamine-induced increase in phagocytosing microglia was $9.2 \pm 0.4\%$, and, thus, in a similar range like histamine-responding microglia in Ca^{2+} imaging experiments. Next we used *Hrh* isoform-specific agonists to identify which receptor isoform responsible for the histamine-induced stimulation of microglial phagocytosis, and that histamine stimulates microglial phagocytosis via *Hrh1* ($3.24 \pm 2.38/3.77$; $n = 34$; $p < 0.0001$), but not by *Hrh2* ($1.25 \pm 0.48/1.93$; $n = 33$ VF; $p > 0.9999$), *Hrh3* ($1.67 \pm 0.58/2.01$; $n = 28$ VF; $p = 0.0357$) or *Hrh4* ($1.86 \pm 1.41/2.26$; $n = 15$ VF; $p = 1.1873$) activation. We further verified these results by blockade of *Hrh1*. Cortical slices were incubated with histamine and *Hrh1* specific antagonist which blocked the histamine-induced stimulation of phagocytosis ($1.45 \pm 0.73/1.81$; $n = 44$ VF; $p > 0.9999$). We also tested whether putatively secondary purinergic signal affects microglial phagocytic activity. The stimulating effect of histamine was completely abolished by the *P2ry12* blocker AR-C69931 ($0.7 \pm 0.28/1.61$; $n = 45$ VF). Similarly, in the presence of the *P2ry12* blocker, the *Hrh1* specific agonist 2-PEA did not potentiate microglia phagocytic activity ($0.75 \pm 0.43/1.92$; $n = 45$ VF), suggesting that histamine-evoked stimulation of microglial phagocytosis depends on microglial *P2ry12*.

In conclusion, histamine acts indirectly on microglial Ca^{2+} levels and phagocytic activity via astrocyte histamine receptor-controlled purinergic signaling.

Freshly isolated microglia(coverslips)



Cortical microglia(*in situ*)

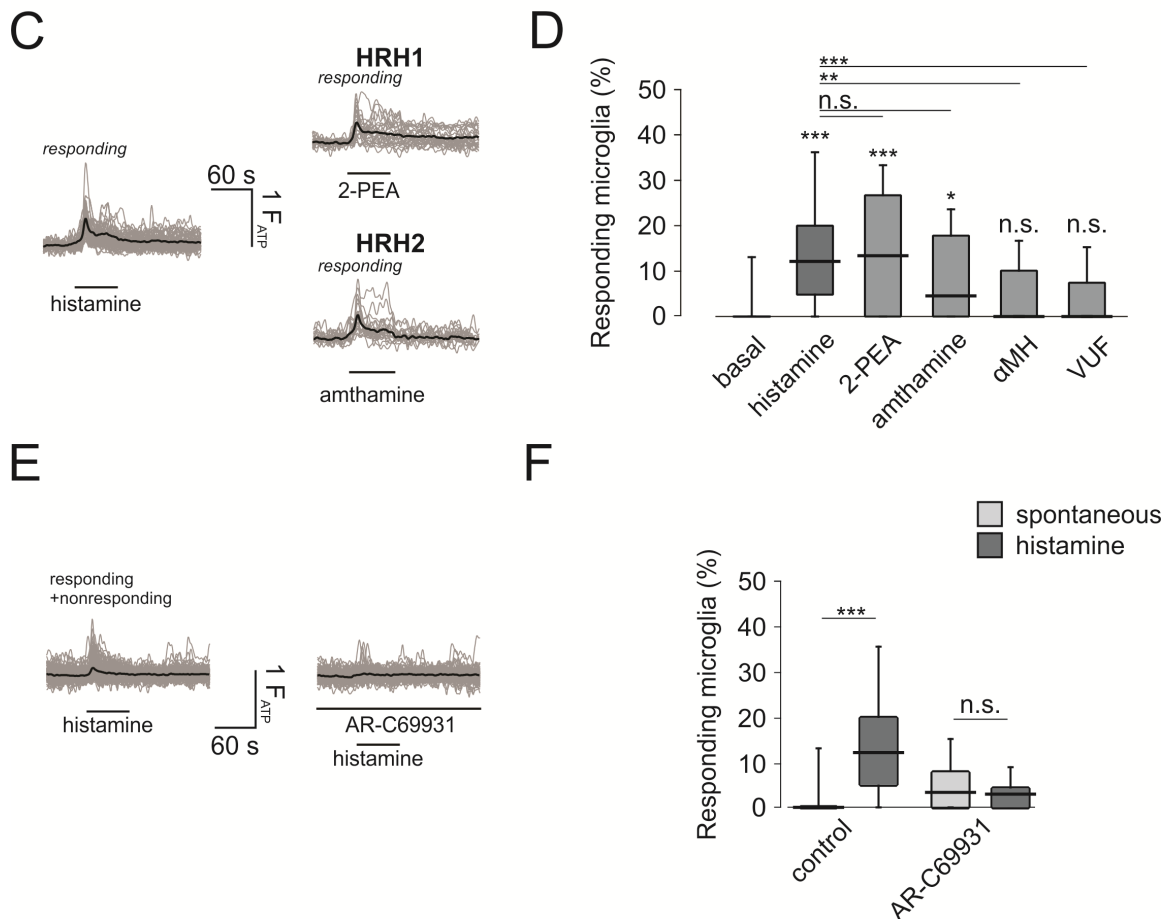


Figure 2: Histamine triggers microglial intracellular Ca^{2+} responses via *P2ry12* and *Hrh2*.

A. Overlay of intracellular Ca^{2+} responses from microglia in response to histamine (100 μ M, left) and amthamine (*Hrh2* agonist; 10 μ M, right). The black trace is the average response of all responding cells (gray).

B. Summary of microglia Ca^{2+} responses upon histamine (100 μ M), 2-PEA (*Hrh1* agonist; 100

μM), amthamine (*Hrh2* agonist; 10 μM), α -methylhistamine (αMH ; *Hrh3* agonist; 1 μM) or VUF10460/VUF 10460 (VUF; *Hrh4* agonist; 10 μM) and under basal conditions. Note that only *Hrh2* activation evoked microglial Ca^{2+} responses similar to histamine. Significance statement above the bars is from comparison against basal conditions.

C. Overlay of intracellular Ca^{2+} responses from in situ cortical microglia responding to histamine, a *Hrh1*- (2-PEA, 100 μM) and a *Hrh2*- (Amthamine; 10 μM) specific agonist. Black traces indicate the average response of all responding cells (gray).

D. Summary of the responding microglia from experiments shown in C, including those with *Hrh3*- (α -methylhistamine; 10 μM) and *Hrh4*- (VUF10460; 10 μM) specific agonists.

E. Overlay of intracellular Ca^{2+} responses from in situ cortical microglia responding to histamine in the presence or absence of the *P2ry12* inhibitor AR-C69931 (1 μM). Black traces indicate the average response of all responding cells (gray). Note that unlike in the other figures, both responding and non-responding traces are shown in these plots.

F. Summary of the responding microglia from experiments shown in E.

Data are presented as median \pm 25%/75% percentile, Box Plots indicate the median (black line) as well as the 25-75% (box) and 10-90% (whiskers) percentiles. Statistical significance was tested by a Kruskal-Wallis test followed by Dunn's multiple comparisons test and is indicated as followed: n.s., $p \geq 0.05$; *, $p \leq 0.05$; **, $p \leq 0.01$, ***, $p \leq 0.001$.

(Figure adapted from Xia *et al.*, 2021).

2.4 Further scientific questions

The studies of Xia *et al.* (2021) investigated which receptors and pathways are involved in microglial responses upon brain histamine. We presented for the first time that the direct responses of microglial cells upon changes in histamine concentration in different brain regions, visualized by Ca²⁺ imaging, directly in a *Hrh2* dependent manner and indirectly through interaction with astrocytes, mediated by *Hrh1* signaling, ATP release from astrocytes and interaction with microglial *P2ry12*. Moreover, in a similar mechanism that histamine also increases phagocytic activity of microglia via *Hrh1*- and *P2ry12*-mediated signaling pathways *in situ*.

In the cortex, we found that the majority of microglial Ca²⁺ level changes upon histamine application are indirectly mediated by *Hrh1* activation on astrocytes which subsequently communicate with microglia via ATP/ADP and *P2ry12*. This kind of pangling communication turned out to be also responsible for the stimulatory effect of histamine on microglial phagocytosis. Our data therefore confirm the notion that neurotransmitter in the brain rarely act in a simple, linear manner on autonomous cells but rather initiate or modulate sophisticated cellular networks consisting of different cell types.

Although microglia *in situ* are much more physiological than cultures, there is still the missing blood flow and the slicing procedure which could microglia shift towards a more non-physiological, activated state. However, the pathway we have demonstrated in the current study, depends on astrocytes that primarily respond to histamine via *Hrh1*, whereas the majority of microglia-responded putatively secondary- to histamine in a *P2ry12*-dependent fashion. As microglial *P2ry12* expression does not seem to vary between different microglia preparations, it seems unlikely that results will differ largely when experiments were done *in vivo*. Furthermore, *in vivo* recordings require a huge set of material, experience and permissions from the local authorities which is not available at the moment. For testing microglia responses upon histamine under more physiological conditions, we added experiments that were performed at 37°C. There were no significant differences in basal or histamine responses when experiments were performed at 37°C compared with RT group.

Notably, we also observed in the present study that a very low intrinsic microglial expression of *Hrh2*. The application of the *Hrh2*-specific agonist amthamine evoked intracellular Ca²⁺ elevations in both brain slices and freshly isolated cortical microglia in a comparable population of the cells. In addition, only blocking *Hrh2* instead of other *Hrh* isoforms could inhibit the histamine response on isolated microglia. These findings also confirmed many previous transcriptomic observations on a functional level (Grabert *et al.*, 2016, Butovsky *et al.*, 2014, Hickman *et al.*, 2013, Zhang *et al.*, 2014). It remains still elusive, however, which role microglial *Hrh2* receptors might have

at physiological and non-physiological states. The treatment of acute brain slices with amthamine had no effect on the phagocytic activity of microglia, suggesting that the endogenous *Hrh2* of microglia has little impact on controlling phagocytic activity. One possible reason could be that in healthy conditions the expression of *Hrh2* is very low and can be ignored. However, microglial cells are more sensitive to histamine under disease conditions. One previous paper published from our group illustrated that Lipopolysaccharide (LPS) treatment significantly increased the response of microglia to histamine (Pannell *et al.*, 2014). Another possibility could be that *Hrh2* affects other physiological properties of microglia rather than phagocytosis, such as ramification (Frick *et al.*, 2016). Also, we did not completely capture all microglia histamine responses by monitoring intracellular Ca^{2+} level changes. The latter case could happen if most of the membrane-accessible *Hrh2* protein was located rather in microglial processes than the soma from where we obtained fluorescence level changes of the transgenic GCaMP indicator.

There have been multiple studies focusing on the effect of histamine on the phagocytosis of microglia. However, none of the reports focused on the potential intervention of neurons or astrocytes in response to microglia. Only one *in vivo* study which was carried out by Rocha *et al* (Rocha *et al.*, 2016) investigated the relationship between histamine and microglia phagocytosis. They observed that stereotactic co-injection of histamine can increase the effect of microglia on the substantia nigra containing phosphatidylcholine liposomes phagocytosis, suggesting the stimulating effect of the phagocytic activity of microglia through histamine. These results are consistent with our findings, although the interaction between histamine and astrocytes has not been directly clarified.

Our study revealed that microglia in different brain regions respond differently to histamine. Interestingly, the response of microglia is increased in brain regions with a larger proportion of white matter, such as the thalamus and corpus callosum. In the thalamus, the *Hrh* subtype specific activation pattern is similar to that in the cortex, indicating that it is not the internal expression of the *Hrh* subtype of microglia, but the communication between microglia and non-microglia in different brain regions that mediate the microglial response to histamine. It would be extremely interesting to shed light on this question.

Histamine, as a modulatory neurotransmitter, is associated with many brain functions like Neuroendocrine regulation, drinking water intake regulation, temperature regulation, learning and memory, motor movement and aggressive behavior. Abnormalities in the histaminergic system are associated with many brain diseases like Alzheimer's disease, epilepsy, Parkinson's syndrome, and ischemic brain disease. Microglia are involved in many physiological and almost all pathological processes of the central nervous system, and their ability to adjust or stimulate histaminergic systems through astrocytes and purinergic pathways may have important effects on their behavior. Therefore, we conclude that histamine-related processes in the

brain may be related to the activity of microglia through the purinergic pathway, this unexpected connection between astrocytes and microglia may be critical to the development of new immuno-related therapies in the future.

2.5 References

- APOLLONI, S., FABBRIZIO, P., AMADIO, S., NAPOLI, G., VERDILE, V., MORELLO, G., IEMMOLO, R., ARONICA, E., CAVALLARO, S. & VOLONTE, C. (2017), "Histamine Regulates the Inflammatory Profile of SOD1-G93A Microglia and the Histaminergic System Is Dysregulated in Amyotrophic Lateral Sclerosis", *Front Immunol*, Vol. 81689.
- BADER, M. F., TAUPENOT, L., ULRICH, G., AUNIS, D. & CIESIELSKI-TRESKA, J. (1994), "Bacterial endotoxin induces $[Ca^{2+}]_i$ transients and changes the organization of actin in microglia", *Glia*, Vol. 11 No. 4, pp. 336-44.
- BOUCSEIN, C., ZACHARIAS, R., FARBER, K., PAVLOVIC, S., HANISCH, U. K. & KETTENMANN, H. (2003), "Purinergic receptors on microglial cells: functional expression in acute brain slices and modulation of microglial activation in vitro", *Eur J Neurosci*, Vol. 17 No. 11, pp. 2267-76.
- BUTOVSKY, O., JEDRYCHOWSKI, M. P., MOORE, C. S., CIALIC, R., LANSER, A. J., GABRIELY, G., KOEGLSPERGER, T., DAKE, B., WU, P. M., DOYKAN, C. E., FANEK, Z., LIU, L., CHEN, Z., ROTHSTEIN, J. D., RANSOHOFF, R. M., GYGI, S. P., ANTEL, J. P. & WEINER, H. L. (2014), "Identification of a unique TGF-beta-dependent molecular and functional signature in microglia", *Nat Neurosci*, Vol. 17 No. 1, pp. 131-43.
- FARBER, K. & KETTENMANN, H. (2006), "Functional role of calcium signals for microglial function", *Glia*, Vol. 54 No. 7, pp. 656-65.
- FRICK, L., RAPANELLI, M., ABBASI, E., OHTSU, H. & PITTENGER, C. (2016), "Histamine regulation of microglia: Gene-environment interaction in the regulation of central nervous system inflammation", *Brain Behav Immun*, Vol. 57326-337.
- GRABERT, K., MICHOEL, T., KARAVOLOS, M. H., CLOHISEY, S., BAILLIE, J. K., STEVENS, M. P., FREEMAN, T. C., SUMMERS, K. M. & MCCOLL, B. W. (2016), "Microglial brain region-dependent diversity and selective regional sensitivities to aging", *Nat Neurosci*, Vol. 19 No. 3, pp. 504-16.
- HAAS, H. & PANULA, P. (2003), "The role of histamine and the tuberomammillary nucleus in the nervous system", *Nat Rev Neurosci*, Vol. 4 No. 2, pp. 121-30.
- HANISCH, U. K. & KETTENMANN, H. (2007), "Microglia: active sensor and versatile effector cells in the normal and pathologic brain", *Nat Neurosci*, Vol. 10 No. 11, pp. 1387-94.
- HICKMAN, S. E., KINGERY, N. D., OHSUMI, T. K., BOROWSKY, M. L., WANG, L. C., MEANS, T. K. & EL, K. J. (2013), "The microglial sensome revealed by direct RNA sequencing", *Nat Neurosci*, Vol. 16 No. 12, pp. 1896-905.
- IIDA, T., YOSHIKAWA, T., MATSUZAWA, T., NAGANUMA, F., NAKAMURA, T., MIURA, Y., MOHSEN, A. S., HARADA, R., IWATA, R. & YANAI, K. (2015), "Histamine H3 receptor in primary mouse microglia inhibits chemotaxis,

phagocytosis, and cytokine secretion", *Glia*, Vol. 63 No. 7, pp. 1213-25.

INOUE, K. (2002), "Microglial activation by purines and pyrimidines", *Glia*, Vol. 40 No. 2, pp. 156-63.

JUNG, S., PFEIFFER, F. & DEITMER, J. W. (2000), "Histamine-induced calcium entry in rat cerebellar astrocytes: evidence for capacitative and non-capacitative mechanisms", *J Physiol*, Vol. 527 Pt 3549-61.

JURIC, D. M., KRZAN, M. & LIPNIK-STANGELJ, M. (2016), "Histamine and astrocyte function", *Pharmacol Res*, Vol. 111774-783.

KETTENMANN, H., HANISCH, U. K., NODA, M. & VERKHRATSKY, A. (2011), "Physiology of microglia", *Physiol Rev*, Vol. 91 No. 2, pp. 461-553.

MOLLER, T. (2002), "Calcium signaling in microglial cells", *Glia*, Vol. 40 No. 2, pp. 184-94.

NIKODEMOVA, M. & WATTERS, J. J. (2012), "Efficient isolation of live microglia with preserved phenotypes from adult mouse brain", *J Neuroinflammation*, Vol. 9147.

NIMMERJAHN, A., KIRCHHOFF, F. & HELMCHEN, F. (2005), "Resting microglial cells are highly dynamic surveillants of brain parenchyma in vivo", *Science*, Vol. 308 No. 5726, pp. 1314-8.

PANNELL, M., MEIER, M. A., SZULZEWSKY, F., MATYASH, V., ENDRES, M., KRONENBERG, G., PRINZ, V., WAICZIES, S., WOLF, S. A. & KETTENMANN, H. (2016), "The subpopulation of microglia expressing functional muscarinic acetylcholine receptors expands in stroke and Alzheimer's disease", *Brain Struct Funct*, Vol. 221 No. 2, pp. 1157-72.

PANNELL, M., SZULZEWSKY, F., MATYASH, V., WOLF, S. A. & KETTENMANN, H. (2014), "The subpopulation of microglia sensitive to neurotransmitters/neurohormones is modulated by stimulation with LPS, interferon-gamma, and IL-4", *Glia*, Vol. 62 No. 5, pp. 667-79.

PANULA, P. & NUUTINEN, S. (2013), "The histaminergic network in the brain: basic organization and role in disease", *Nat Rev Neurosci*, Vol. 14 No. 7, pp. 472-87.

PASSANI, M. B., BACCIOTTINI, L., MANNAIONI, P. F. & BLANDINA, P. (2000a), "Central histaminergic system and cognition", *Neurosci Biobehav Rev*, Vol. 24 No. 1, pp. 107-13.

POCOCK, J. M. & KETTENMANN, H. (2007), "Neurotransmitter receptors on microglia", *Trends Neurosci*, Vol. 30 No. 10, pp. 527-35.

ROCHA, S. M., SARAIVA, T., CRISTOVAO, A. C., FERREIRA, R., SANTOS, T., ESTEVES, M., SARAIVA, C., JE, G., CORTES, L., VALERO, J., ALVES, G., KLIBANOV, A., KIM, Y. S. & BERNARDINO, L. (2016), "Histamine induces microglia activation and dopaminergic neuronal toxicity via H1 receptor activation", *J Neuroinflammation*, Vol. 13 No. 1, pp. 137.

SCHIPKE, C. G., BOUCSEIN, C., OHLEMEYER, C., KIRCHHOFF, F. & KETTENMANN, H. (2002), "Astrocyte Ca²⁺ waves trigger responses in microglial cells in brain slices", *FASEB J*, Vol. 16 No. 2, pp. 255-7.

THANGAM, E. B., JEMIMA, E. A., SINGH, H., BAIG, M. S., KHAN, M.,

- MATHIAS, C. B., CHURCH, M. K. & SALUJA, R. (2018), "The Role of Histamine and Histamine Receptors in Mast Cell-Mediated Allergy and Inflammation: The Hunt for New Therapeutic Targets", *Front Immunol*, Vol. 91873.
- VERDERIO, C. & MATTEOLI, M. (2001), "ATP mediates calcium signaling between astrocytes and microglial cells: modulation by IFN-gamma", *J Immunol*, Vol. 166 No. 10, pp. 6383-91.
- VITRAC, C. & BENOIT-MARAND, M. (2017), "Monoaminergic Modulation of Motor Cortex Function", *Front Neural Circuits*, Vol. 1172.
- WENDT, S., MARICOS, M., VANA, N., MEYER, N., GUNEYKAYA, D., SEMTNER, M. & KETTENMANN, H. (2017), "Changes in phagocytosis and potassium channel activity in microglia of 5xFAD mice indicate alterations in purinergic signaling in a mouse model of Alzheimer's disease", *Neurobiol Aging*, Vol. 5841-53.
- WOLF, S. A., BODDEKE, H. W. & KETTENMANN, H. (2017), "Microglia in Physiology and Disease", *Annu Rev Physiol*, Vol. 79619-643.
- XIA, P., LOGIACCO, F., HUANG, Y., KETTENMANN, H. & SEMTNER, M. (2021), "Histamine triggers microglial responses indirectly via astrocytes and purinergic signaling", *Glia*, Vol. 69 No. 9, pp. 2291-2304.
- ZHANG, Y., CHEN, K., SLOAN, S. A., BENNETT, M. L., SCHOLZE, A. R., O'KEEFFE, S., PHATNANI, H. P., GUARNIERI, P., CANEDA, C., RUDERISCH, N., DENG, S., LIDDELOW, S. A., ZHANG, C., DANEMAN, R., MANIATIS, T., BARRES, B. A. & WU, J. Q. (2014), "An RNA-sequencing transcriptome and splicing database of glia, neurons, and vascular cells of the cerebral cortex", *J Neurosci*, Vol. 34 No. 36, pp. 11929-47.

3. Statutory Declaration

“I, Pengfei Xia, by personally signing this document in lieu of an oath, hereby affirm that I prepared the submitted dissertation on the topic Brain histamine acts on microglia mainly via astrocytes (Gehirnhistamin wirkt auf Mikroglia hauptsächlich über Astrozyten), independently and without the support of third parties, and that I used no other sources and aids than those stated.

All parts which are based on the publications or presentations of other authors, either in letter or in spirit, are specified as such in accordance with the citing guidelines. The sections on methodology (in particular regarding practical work, laboratory regulations, statistical processing) and results (in particular regarding figures, charts and tables) are exclusively my responsibility.

Furthermore, I declare that I have correctly marked all of the data, the analyses, and the conclusions generated from data obtained in collaboration with other persons, and that I have correctly marked my own contribution and the contributions of other persons (cf. declaration of contribution). I have correctly marked all texts or parts of texts that were generated in collaboration with other persons.

My contributions to any publications to this dissertation correspond to those stated in the below joint declaration made together with the supervisor. All publications created within the scope of the dissertation comply with the guidelines of the ICMJE (International Committee of Medical Journal Editors; www.icmje.org) on authorship. In addition, I declare that I shall comply with the regulations of Charité – Universitätsmedizin Berlin on ensuring good scientific practice.

I declare that I have not yet submitted this dissertation in identical or similar form to another Faculty.

The significance of this statutory declaration and the consequences of a false statutory declaration under criminal law (Sections 156, 161 of the German Criminal Code) are known to me.”

Date

Signature

4. Declaration of your own contribution to the publication

Pengfei Xia contributed the following to the below listed publications:

Authors: Pengfei Xia, Francesca Logiacco, Yimin Huang, Helmut Kettenmann*, Marcus Semtner*

*equally contributed

Title: Histamine triggers microglial responses indirectly via astrocytes and purinergic signaling

Journal: Glia

Publication year: 2021

Contributions (in detail):

Helmut Kettenmann and Marcus Semtner conceptualized and supervised the study.

This work was supported by the Helmholtz-Gemeinschaft, Zukunftsthema "Immunology and Inflammation" (ZT-0027) and by the Einstein-Stiftung.

Pengfei Xia Performed and analysed the live cell Ca^{2+} imaging (Figure 1, Figure 2A-B, E-F, Figure 3, Figure 4, Suppl.Figure 2, Suppl.Figure 3, Suppl.Figure 7), immunohistochemistry analysis (Suppl.Figure 6), in situ phagocytosis assay (Figure 5, Suppl.Figure 4).

Francesca Logiacco performed and analysed the 2-photon live-cell Ca^{2+} imaging (Figure 2C-D).

Yimin Huang helped to perform the phagocytosis assay and the Imaris analysis (Suppl.Figure 5).

Marcus Semtner selected and analysis the RNA-sequencing/microarray datasets for meta-analysis (Suppl.Figure 1).

Pengfei Xia and Marcus Semtner discussed the data and designed the figures. Helmut Kettenmann, Marcus Semtner and Pengfei Xia wrote the manuscript with input from all other authors.

Signature, date and stamp of first supervising university professor / lecturer

Signature of doctoral candidate

5. Excerpt of Journal Summary List “Neurosciences”

Journal Data Filtered By: **Selected JCR Year: 2019** Selected Editions: SCIE, SSCI
 Selected Categories: **“NEUROSCIENCES”** Selected Category Scheme: WoS
Gesamtanzahl: 271 Journale

Rank	Full Journal Title	Total Cites	Journal Impact Factor	Eigenfactor Score
1	NATURE REVIEWS NEUROSCIENCE	42,809	33.654	0.055400
2	NATURE NEUROSCIENCE	62,933	20.071	0.144390
3	BEHAVIORAL AND BRAIN SCIENCES	9,395	17.333	0.008170
4	TRENDS IN COGNITIVE SCIENCES	27,705	15.218	0.036050
5	JOURNAL OF PINEAL RESEARCH	10,537	14.528	0.009430
6	NEURON	95,056	14.415	0.199640
7	ACTA NEUROPATHOLOGICA	21,908	14.251	0.040740
8	TRENDS IN NEUROSCIENCES	20,011	12.891	0.021220
9	Annual Review of Neuroscience	13,215	12.547	0.012740
10	MOLECULAR PSYCHIATRY	22,227	12.384	0.054730
11	Nature Human Behaviour	2,457	12.282	0.014190
12	BIOLOGICAL PSYCHIATRY	44,016	12.095	0.053910
13	BRAIN	53,282	11.337	0.067050
14	SLEEP MEDICINE REVIEWS	8,077	9.613	0.013000
15	Molecular Neurodegeneration	4,933	9.599	0.011840
16	PROGRESS IN NEUROBIOLOGY	12,791	9.371	0.011250
17	FRONTIERS IN NEUROENDOCRINOLOGY	4,491	9.059	0.007050
18	ANNALS OF NEUROLOGY	37,304	9.037	0.044120
19	NEUROSCIENCE AND BIOBEHAVIORAL REVIEWS	28,873	8.330	0.051900
20	Neurology-Neuroimmunology & Neuroinflammation	2,232	7.724	0.008400
21	NEUROPATHOLOGY AND APPLIED NEUROBIOLOGY	3,992	7.500	0.005960

Rank	Full Journal Title	Total Cites	Journal Impact Factor	Eigenfactor Score
22	Neurobiology of Stress	1,055	7.197	0.003840
23	NEUROPSYCHOPHARMACOLOGY	26,281	6.751	0.040680
24	npj Parkinsons Disease	662	6.750	0.002500
25	BRAIN BEHAVIOR AND IMMUNITY	16,285	6.633	0.028560
26	Brain Stimulation	6,537	6.565	0.015580
27	NEUROSCIENTIST	5,188	6.500	0.007220
28	Acta Neuropathologica Communications	4,070	6.270	0.014730
29	CURRENT OPINION IN NEUROBIOLOGY	14,959	6.267	0.028730
30	Alzheimers Research & Therapy	3,876	6.116	0.011650
31	Neurotherapeutics	4,998	6.035	0.009520
32	GLIA	14,220	5.984	0.017250
33	NEUROIMAGE	102,632	5.902	0.125360
34	Annual Review of Vision Science	601	5.897	0.003700
35	Molecular Autism	2,510	5.869	0.007450
36	Journal of Neuroinflammation	13,709	5.793	0.025870
37	Translational Stroke Research	2,274	5.780	0.004520
38	JOURNAL OF CEREBRAL BLOOD FLOW AND METABOLISM	19,492	5.681	0.024230
39	JOURNAL OF NEUROSCIENCE	167,114	5.673	0.181170
40	BRAIN PATHOLOGY	5,308	5.568	0.007020
41	Translational Neurodegeneration	1,030	5.551	0.002790
42	NEURAL NETWORKS	14,065	5.535	0.018910
43	PAIN	37,753	5.483	0.035730

6. Publication



Received: 3 February 2021 | Revised: 17 May 2021 | Accepted: 19 May 2021
DOI: 10.1002/glia.24039



WILEY

RESEARCH ARTICLE

Histamine triggers microglial responses indirectly via astrocytes and purinergic signaling

Pengfei Xia^{1,2} | Francesca Loggiacco^{1,3} | Yimin Huang^{1,2} |
Helmut Kettenmann^{1,4} | Marcus Semtner¹

¹Cellular Neurosciences, Max-Delbrück-Center for Molecular Medicine in the Helmholtz Association, Berlin, Germany

²Charité-Universitätsmedizin, Berlin, Germany

³Department of Biology, Chemistry, and Pharmacy, Freie Universität Berlin, Berlin, Germany

⁴Shenzhen Institute of Advanced Technology, Chinese Academy of Sciences, Shenzhen, China

Correspondence

Marcus Semtner, Cellular Neurosciences, Max-Delbrück-Center for Molecular Medicine in the Helmholtz Association, 13125 Berlin, Germany.
Email: marcus.semtner@mdc-berlin.de

Funding information

Einstein-Stiftung; Helmholtz-Gemeinschaft, Zukunftsthema "Immunology and Inflammation", Grant/Award Number: ZT-0027

Abstract

Histamine is a monoaminergic neurotransmitter which is released within the entire brain from ascending axons originating in the tuberomammillary nucleus in a sleep state-dependent fashion. Besides the modulation of neuronal firing patterns, brain histamine levels are also thought to modulate functions of glial cells. Microglia are the innate immune cells and professional phagocytes of the central nervous system, and histamine was previously shown to have multiple effects on microglial functions in health and disease. Isolated microglia respond only to agonists of the *Hrh2* subtype of histamine receptors (*Hrh*), and the expression of that isoform is confirmed by a metadata analysis of microglia transcriptomes. When we studied the effect of the histamine receptor isoforms in cortical and thalamic microglia by *in situ live cell* Ca^{2+} imaging using a novel, microglia-specific indicator mouse line, microglial cells respond to external histamine application mainly in a *Hrh1*-, and to a lower extent also in a *Hrh2*-dependent manner. The *Hrh1* response was sensitive to blockers of purinergic *P2ry12* receptors, and since *Hrh1* expression was predominantly found in astrocytes, we suggest that the *Hrh1* response in microglia is mediated by astrocyte ATP release and activation of *P2ry12* receptors in microglia. Histamine also stimulates microglial phagocytic activity via *Hrh1*- and *P2ry12*-mediated signaling. Taken together, we provide evidence that histamine acts indirectly on microglial Ca^{2+} levels and phagocytic activity via astrocyte histamine receptor-controlled purinergic signaling.

KEYWORDS

astrocyte, calcium, histamine, *Hrh*, microglia, phagocytosis

1 | INTRODUCTION

Histamine is a bioactive amine known to regulate many physiological processes in the periphery, such as allergic reactions, gastric acid

secretion, and itch sensation (Thangam et al. (2018)). In the central nervous system (CNS), histamine is synthesized by L-histidine decarboxylase (HDC)-expressing neurons which are localized in the tuberomammillary nucleus (TMN) from where they send axonal projections towards essentially all brain (Haas & Panula, 2003; Panula & Nuutinen, 2013). Histamine neurons are pacemakers that display

Helmut Kettenmann and Marcus Semtner should be considered shared senior author.

This is an open access article under the terms of the Creative Commons Attribution-NonCommercial-NoDerivs License, which permits use and distribution in any medium, provided the original work is properly cited, the use is non-commercial and no modifications or adaptations are made.
© 2021 The Authors. *GLIA* published by Wiley Periodicals LLC.



regular spontaneous firing patterns at low frequency which are correlated to sleep/wake rhythm with upregulation of histamine release during wakefulness (Vitrac & Benoit-Marand, 2017). Abnormalities in brain histamine release are increasingly appreciated as potential contributors to brain pathologies like Parkinson's disease, Huntington's disease, Alzheimer's disease, narcolepsy, and drug addiction (Panula & Nuutinen, 2013).

Histamine action is mediated by signaling downstream of the four mammalian histamine receptor isoforms (*Hrh1-Hrh4*) which are $G\alpha_q$ (*Hrh1*), $G\alpha_s$ (*Hrh2*), or $G\alpha_i$ (*Hrh3* and *Hrh4*) protein-coupled receptors. Recent transcriptomic and proteomic approaches suggest that there is— if at all—only bare expression of *Hrh4* in the central nervous system (Zhang et al., 2014). The predominant isoform in the brain is *Hrh3* which is mainly expressed by neurons and modulates the release of various neurotransmitters, including GABA and acetylcholine (Passani et al., 2000). Consistent with its abundance and strong impact on neurotransmitter release, *Hrh3* is involved in diverse brain functions, such as memory, cognition, appetite, and arousal. *Hrh1* and *Hrh2* are also expressed by neurons at low levels, however, previous gene expression studies and functional observations suggest that these subunits rather serve as modulators of glial functions. Particularly, *Hrh1*, which is the most abundant *Hrh* isoform in astrocytes, modulates various physiological and pathological activities of astrocytes upon brain histamine level changes including energy metabolism, neurotransmitter clearance, neurotrophic activity, and immune responses (Juric et al., 2016).

Microglia are the resident immune cells of the CNS. Their physiological role is to protect the brain from infection and damage, to promote tissue repair and regeneration, and to modulate neurons and other glial cells by secretion of growth factors, cytokines, and other signal molecules (Wolf et al., 2017). In the healthy postnatal brain, microglia are characterized by a ramified morphology, that is, they have a relatively small soma (~10 μm) with cellular processes that branch off and arborize further more distantly from the soma within a defined territory, and they constantly scan their environment for potential insults (Kettenmann et al., 2011). Microglia are the professional phagocytes of the brain being able to eliminate entire cells or cellular substructures. Microglia recognize cells that undergo programmed cell death and they migrate to different regions of the CNS, usually right before or during the peak of programmed cell death (Wolf et al., 2017). The first report on histamine action on microglia was from Bader et al. (1994) who demonstrated via life cell Ca^{2+} imaging that only a subpopulation of primary cultured rat microglia is responsive to histamine application, a notion that was confirmed in a more recent study on freshly isolated and primary cultured mouse microglia (Pannell et al., 2014). Interestingly, the percentage of histamine-responding microglia dramatically increases upon LPS challenge, indicating that microglia can dynamically adjust their sensitivity to histamine, and suggesting that histamine action on microglia might be heterogeneous with regard to certain physiological and pathophysiological conditions. There are various controversial results of microglial *Hrh* expression and its functional impact. Indeed, histamine was reported to stimulate microglial phagocytic activity *in vitro* and *in situ* in a *Hrh1*-dependent manner (Rocha et al., 2016). Another study

demonstrated an inhibitory effect of histamine on microglial phagocytosis *in vitro* via *Hrh3* (Iida et al., 2015). Further controversy is about microglial migration which was shown to be accelerated by histamine in a *Hrh4*-dependent fashion and in another study inhibited by *Hrh1* and *Hrh2* (Apolloni et al., 2017). In the present study, we used a novel microglia-specific Ca^{2+} indicator mouse model to investigate microglial Ca^{2+} elevations upon histamine and *Hrh*-specific agonists in cortex and thalamus. We provide evidence for functional *Hrh2*, but not *Hrh1*, *Hrh3*, or *Hrh4* expression on microglia and demonstrate that *Hrh1* in astrocytes and microglial *P2ry12* are involved in histamine action on microglia *in situ*.

2 | MATERIALS AND METHODS

2.1 | Animals

This study was carried out at the Max Delbrück Center for Molecular Medicine (MDC) in strict accordance with the guidelines of the European Communities Council Directive for care of laboratory animals (86/609/EEC) and of the State of Berlin's Office for Health and Social Affairs (Landesamt für Gesundheit und Soziales, LaGeSo), as well as internal MDC guidelines. Experimental protocols were approved under license (X9005/18, X9023/12, A0376/17). Animals were bred and maintained at the MDC animal facility in a temperature- and humidity-controlled environment with a 12 h light-dark cycle and *ad libitum* access to food and water. The mouse strains Csf1R-2A-GCaMP6m and Csf1R-2A-mCherry-2A-GCaMP6m are novel, microglia-specific calcium indicator lines which are described in another paper from our lab (Loggiacco et al., *in press*). hGFAP-mRFP transgenic mice express the red fluorescent protein (mRFP) in astrocytes under control of the promoter for human glial fibrillary acidic protein (GFAP) (Hirrlinger et al., 2005). We pooled male and female mice in all experiments.

2.2 | Chemicals

The following substances were used in the present study: histamine dihydrochloride (Sigma-Aldrich; 100 μM), 2-pyridylethylamine dihydrochlorid (2-PEA; R&D Systems; 100 μM), amthamine (Enzo; 10 μM), α -methylhistamine (αMH ; Biomol; 1 μM), VUF 10460 (Biomol; 10 μM), cetirizine (Sigma-Aldrich; 10 μM), Tiotidine (R&D Systems; 10 μM), carbinine (Sigma-Aldrich; 10 μM), AR-C69931 tetrasodium salt (Tocris, Bio-Techne GmbH, Wiesbaden-Nordenstadt; 1 μM). All chemicals were obtained as powder and initially stock-diluted at a 1,000 fold concentration in DMSO or H_2O .

2.3 | Acute brain slice preparation

Acute cortical brain slices from adult male and female C57BL/6, Csf1R-2A-GCaMP6m or Csf1R-2A-mCherry-2A-GCaMP6m mice

(P40–P90) were prepared as previously described (Boucsein et al., 2003). In brief, adult mice were killed by cervical dislocation. After the brain was extracted, the cerebellum and the olfactory bulbs were gently removed and transferred to ice-cold slicing solution (230 mM sucrose, 26 mM NaHCO₃, 2.5 mM KCl, 1.25 mM NaH₂PO₄, 10 mM MgSO₄, 0.5 mM CaCl₂, 10 mM D-glucose; pH 7.4; saturated with carbogen: 95% O₂, 5% CO₂) to generate 140 μ m (phagocytosis assay) or 250 μ m (Ca²⁺ imaging) thick coronal slices using a vibratome (HM650V, Thermo Scientific). Slices were immediately transferred into artificial cerebrospinal fluid (ACSF): 134 mM NaCl, 26 mM NaHCO₃, 2.5 mM KCl, 1.26 mM K₂HPO₄, 1.3 mM MgCl₂, 2 mM CaCl₂, 10 mM D-glucose; pH 7.4 which was saturated with carbogen (95% O₂, 5% CO₂) at room temperature. The brain slices were kept in ACSF at least 1 h until further treatment.

2.4 | Preparation of freshly isolated microglia

Microglia from adult C57BL/6 mice (P49–P90) were acutely isolated and purified for calcium imaging using magnetic-activated cell sorting (MACS) as described previously (Nikodemova & Watters, 2012). Briefly, adult mice were sacrificed by transcardial perfusion with ice-cold phosphate-buffered solution (PBS) under deep anesthesia to remove the blood. The brain was removed and only the cortex was dissected into Miltenyi Biotec adult brain Dissociation Kit (Trypsin) and dissociated in the gentleMACS Octo Dissociator with heaters (Miltenyi Biotec) for 30 min. After dissociation, the suspension was passed through a MACS SmartStrainer (70 μ m) followed by centrifugation for 1 min at 300 g and 4°C to obtain a single cell suspension. The cell suspension was then homogenized and resuspended in debris removal solution (Miltenyi Biotec). A layer of PBS was very gently applied on top and centrifuged at 3000g, 4°C for 10 min with full acceleration and full brake. The cells were washed and resuspended in MACS-buffer (PBS, 0.5% bovine serum albumin, 2 mM EDTA) and stained with CD11b magnetic Microbeads (Miltenyi Biotec) at 4°C for 15 min. Labeled CD11b-positive cells (microglia) within the large-sized MACS column were then flushed out and plated onto glass coverslips, followed by incubation in DMEM (Invitrogen, Karlsruhe, Germany) medium for at least 2 h to allow adherence. Ca²⁺ imaging was subsequently carried out as described below.

2.5 | Calcium imaging

Acutely isolated microglial cells were plated on glass coverslips. After 2 h, adhered microglia were incubated for 40 min with 5 μ M Fluo-4/AM (Invitrogen) in standard extracellular solution (150 mM NaCl, 5.4 mM KCl, 0.98 mM MgCl₂, 1.97 mM CaCl₂, 10 mM HEPES, and 10 mM glucose; pH 7.4) at room temperature. Acute brain slices from Csf1R-2A-GCaMP6m mice were only maintained in carbogenized ACSF at RT, while slices (250 μ m) from C57/Bl6 mice were generated and loaded with 10 μ M Fluo4/AM for 1 h at 37°C to stain astrocytes.

Coverslips or brain slices were transferred into a recording chamber constantly perfused with standard extracellular solution (isolated microglia) or carbogenized ACSF (brain slices). The perfusion system was equipped with a perfusion pencil which allowed instant and local application of the test substances, as well as 1 mM ATP (Adenosine-Triphosphate) applied at the end of every recording as control. The flow of the perfusion system was adjusted to 0.5–0.6 ml/min. Before live cell Ca²⁺ imaging, each brain slice/coverslip was first examined using a 5X objective and bright field illumination. For Ca²⁺ recordings, we used a \times 20 objective (Carl Zeiss Microscopy GmbH), a Zyla 5.5 camera (Oxford Instruments), a light-emitting diode illuminator (pE-4,000, CoolLED, Andover, UK) and a standard EGFP filter set. An EPC9 amplifier (HEKA) and TIDA 5.25 software (HEKA) were used to trigger fluorescence excitation and image acquisition. To monitor Ca²⁺ level changes over time, images were taken at a rate of 1 frame per second and an exposure time of 100 ms. For experiments at 37°C, we used an inline heater (Warner Instruments Corp.).

For 2-Photon imaging, we used a custom-built 2-photon microscope consisting of an BX61WI microscope stage (Olympus) equipped with a \times 40 water immersion objective placed on a PD72Z4CA piezo drive (Physik Instrumente), a Chameleon Ultra II laser (Coherent) and GaAsP photomultipliers (Thorlabs). The GCaMP6m protein was excited at a wavelength of 940 nm. Movies were acquired at a sampling rate of one 3D image per second, whereas each 3D image covered seven fields of 160 \times 160 μ m with a z distance of 2 μ m (i.e., total z distance: 40 μ m). ThorImage 8.0 was used to drive the image acquisition during calcium imaging experiments. For offline analysis, each 3D image was subjected to a maximum intensity projection to obtain a 2D movie by using a custom-built procedure in IGOR Pro 6.37 (WaveMetrics). Calcium imaging movies were analyzed using a home-made algorithm in Igor Pro 6.37 (WaveMetrics). For analysis, cell somata which were visible in the presence of ATP at the end of each experiment were selected as ROIs, and the mean relative fluorescence intensity for each ROI and frame was determined to display changes in Ca²⁺ levels over time for each cell. This means that only ATP-responding microglia/astrocytes were taken into the subsequent analysis. Intracellular Ca²⁺ elevations were counted as “responsive” upon application of a substance when the Ca²⁺ response amplitude exceeded a level three times (microglia) or five times (astrocytes) the SD from the baseline that was obtained in the 60 s immediately before application. We averaged the cellular response rates from each slice to obtain one “n” for the subsequent statistical analysis. Recordings with less than five microglia in the view field were excluded from analysis. For the analysis of amplitudes and kinetics of microglial Ca²⁺ responses as well as for averaging histamine responses in the figures (stated as “responding”), we used only “responding” events and excluded non-responders.

2.6 | In situ phagocytosis assay

Phagocytosis assay in acute cortical or thalamic brain slices was conducted as previously described (Wendt et al., 2017). Briefly, coronal brain slices from C57/Bl6 mice were generated and maintained for

2 h at RT in ACSF to recover from the slicing procedure (see above). Subsequently, slices were incubated at 37°C for 1 h with latex beads (4.5 μm diameter, Polysciences, Hirschberg Germany), either only in ACSF or together with the specified histamine or isoform-specific agonists and antagonists; then washed three times in 0.1 M PBS (20 min), fixed with 4% paraformaldehyde for 1 h for subsequent staining and again washed three times in 0.1 M PBS (20 min each). For staining, slices were incubated for 4 h at room temperature in a permeabilization buffer containing 2% Triton X-100 (Carl Roth), 2% bovine serum albumin (Carl Roth), 10% normal donkey serum (EMD Millipore) in 0.1 M PBS (pH 7.4) and then overnight incubated with a goat anti-Iba1 antibody (1:600; clone #5076 Abcam) in dilution buffer (1:10 of permeabilization buffer in 0.1 M PBS) at 4°C. On the next day, slices were incubated for 2 h with the secondary antibody donkey anti-goat Alexa Fluor 647 (1:250; Dianova). After washing, the slices were mounted on glass slides with Aqua Polymount mounting medium (Polysciences). Confocal laser scanning microscopy was performed on a Leica TCS SPE confocal microscope (Leica) using a ×20 oil immersion objective. We acquired 21 μm thick z-stacks at 1.05 μm intervals beginning from the surface of the slice.

Data analysis to assess microglial phagocytic activity was performed using Imaris 6.3.1 (Bitplane). The Iba1-positive volumes of high-resolution SPE confocal microscopy stacks were 3D surface rendered using a software-internal threshold value of 40 AU and a background subtraction (software-internal parameters: 1–3 times, ~90 μm each). Microspheres were detected as spots and counted. All beads having their center located within a given rendered Iba1 volume were considered to be phagocytosed by microglia. The phagocytic index was calculated as: $n_{PM} \cdot 10^4 / V_{Iba1}$ (n_{PM} is the total number of phagocytosed microspheres and V_{Iba1} is the Imaris-rendered volume of Iba1 fluorescence in μm³). Igor Pro 6.37 (WaveMetrics) and Prism 7 (GraphPad Software) were used for subsequent statistical analysis.

2.7 | Metadata analysis

The cell-type-specific expression of *Hrh* isoforms was obtained directly from the website www.brainmaseq.org. Single FPKM values were compiled in IGOR Pro 6.37 and plotted as heat map (Figure S1A; Zhang et al., 2014). For looking into the brain region-specific microglial RNAseq dataset at different ages (Grabert et al., 2016), the normalized data set GSE62420 was downloaded from the GEO site (<https://www.ncbi.nlm.nih.gov/geo/>), and FPKM values of each sample were normalized to the expression of *Hprt* for a proper comparison between different brain regions. *Hrh* and *P2ry12* values were finally compiled in IGOR Pro 6.37 and plotted as heat map. For *Hrh* and *P2ry12* expression in single microglia (Tabula Muris Consortium, 2018), we utilized the online tools on <https://tabula-muris.ds.cbiohub.org/> and exported the resulting plots.

2.8 | Statistical analysis

All data represent the percentage of microglia responding in each brain region from at least three animals per experimental condition.

We applied the Kruskal-Wallis followed by a Dunn's multiple comparison test to calculate significance levels between data sets. Data are given as median ± 25%/75% percentile. Statistical significance levels are represented as n.s.: $p > .05$; *: $p < .05$; **: $p < .01$; ***: $p < .001$.

3 | RESULTS

3.1 | Microglial histamine responses are mediated by *Hrh2* receptors

Microglia were previously shown in vitro to functionally express histamine receptors that mediate downstream cytosolic Ca²⁺ elevations (Pannell et al., 2014). We revisited these findings and determined histamine responses in freshly isolated cortical microglia from C57/Bl6 mice which were loaded with Fluo4/AM to indicate intracellular Ca²⁺ level changes (Figure 1a,b). ATP (1 mM) was applied at the end of each recording and only ATP-responding cells were considered for the subsequent analysis. As microglia are known to display spontaneous Ca²⁺ elevations (Korvers et al., 2016), we first determined the probability of spontaneous events within a minute before histamine application which was observed in $1.13 \pm 0/3.39\%$ of the cells ($n = 3,028$ isolated cells, 54 recordings, 11 mice). In accordance with our published data set, a subpopulation ($5.88 \pm 2.98/8.00\%$; $n = 502$ cells, 15 recordings, 4 mice) of these microglial cells responded to histamine which was a significantly higher rate than spontaneous Ca²⁺ elevations before histamine application ($p = .0021$). Microglial Ca²⁺ responses to histamine had a peak of 0.72 ± 0.16 relative to the responses upon ATP; they were transient and completely reversed to background levels upon wash out.

In the mammalian genome, there are four known histamine receptor isoforms (*Hrh1-4*; Passani et al., 2000). In an attempt to identify the receptor isoform responsible for microglial histamine responses, we used *Hrh* isoform-specific agonists. As shown in Figure 1c,d, freshly isolated microglia selectively responded to the *Hrh2*-specific agonist amthamine (10 μM). $4.17 \pm 2.38/11.83\%$ of the ATP-responding isolated microglia displayed amthamine-evoked Ca²⁺ elevations ($n = 1,345$ cells, 25 recordings, 7 mice) which was similar to the histamine-responding population ($5.88 \pm 2.98/8.00\%$; $p = .9999$) and significantly more than the level of spontaneously active cells ($p = .0016$). *Hrh1* activation by 2-pyridylethylamine dihydrochlorid (2-PEA; 100 μM) did, however, not stimulate Ca²⁺ elevations in freshly isolated microglia as the response rate was similar to basal activity ($2 \pm 0.37/3.75\%$; $n = 962$ cells, 15 recordings, 5 mice; $p = .9999$). There was also no response to *Hrh3* and *Hrh4* activation by α-Methylhistamine (αMH; 1 μM) and VUF 10460 (VUF; 10 μM), respectively (Figure 1d). We therefore conclude that microglia express *Hrh2* receptors which mediate intracellular Ca²⁺ elevations upon histamine application. This conclusion is strongly supported by previously published transcriptomic expression profiles of microglia and other brain cell types. A meta-analysis of several data sets (Figure S1) revealed that indeed *hrh2* is the predominant isoform in microglia whereas *hrh1* is mainly expressed by astrocytes and *hrh3* by neurons (Zhang et al., 2014). Specific expression of *hrh2* in microglial

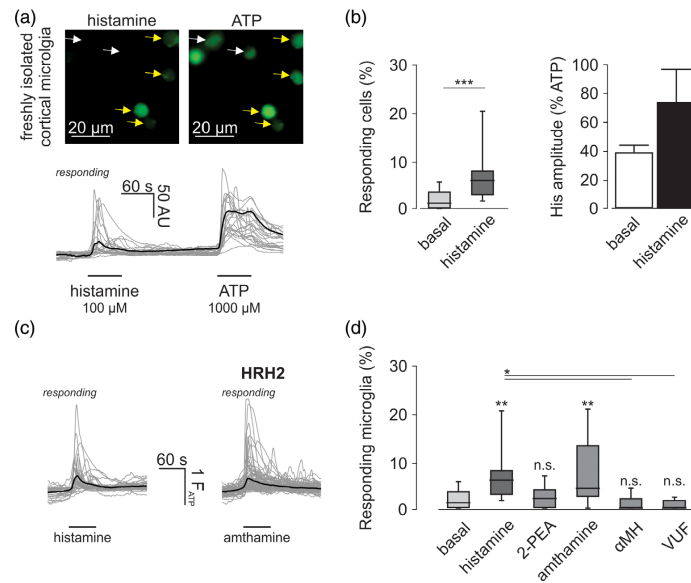


FIGURE 1 Freshly isolated cortical microglia respond to histamine via *Hrh2* activation. (a) Top, representative images from live-cell recordings on adult isolated microglial cells in the presence of histamine (left) and ATP (right). Isolated microglia were obtained from C57/Bl6 cortex via MACS (CD11b) and loaded with Fluo4/AM before recordings. Images were generated by subtraction of the movie frames before substance application from frames in the presence. Histamine-responding microglia are indicated with a yellow arrow, non-responding microglia with a white arrow. Bottom, overlay of intracellular Ca^{2+} responses from cortical histamine-responding microglia. The black trace is the average response of all responding cells (gray). (b) Left, percentage of freshly isolated microglia responding spontaneously or upon histamine application. Right, Average amplitudes of microglial histamine responses normalized to the amplitude of ATP responses. (c) Overlay of intracellular Ca^{2+} responses from microglia in response to histamine (100 μM , left) and amthamine (*Hrh2* agonist; 10 μM , right). The black trace is the average response of all responding cells (gray). (d) Summary of microglia Ca^{2+} responses upon histamine (100 μM), 2-PEA (*Hrh1* agonist; 100 μM), amthamine (*Hrh2* agonist; 10 μM), α -methylhistamine (αMH ; *Hrh3* agonist; 1 μM) or VUF 10460 (VUF; *Hrh4* agonist; 10 μM) and under basal conditions. Note that only *Hrh2* activation evoked microglial Ca^{2+} responses similar to histamine. Significance statement above the bars is from comparison against basal conditions. Box Plots indicate the median (black line) as well as the 25%-75% (box) and 10%-90% (whiskers) percentiles. Statistical significance was tested by a Kruskal-Wallis test followed by Dunn's multiple comparisons test and is indicated as followed: n.s., $p \geq .05$; * $p \leq .05$; ** $p \leq .01$; *** $p \leq .001$. Number of mice/experiments/cells: N(basal) = 11/54/3028; N(histamine) = 8/15/502; N(2-PEA) = 5/15/962; N(amthamine) = 7/25/1345; N(αMH) = 2/5/120; N(VUF) = 1/4/144

cells was also confirmed in many other transcriptomic data sets including the one provided by Grabert et al. (2016); Figure S1B), the Tabula Muris Consortium (2018); Figure S1C, Bowman et al. (2016) and Sala Frigerio et al. (2019)). Taken together, both transcriptomic analysis and live cell investigation of isolated microglia support the notion that *Hrh2* is the only histamine receptor isoform expressed intrinsically in microglial cells and mediates microglial Ca^{2+} responses upon histamine stimulation.

3.2 | A subpopulation of microglia responds to histamine in different brain regions

We applied our novel transgenic Ca^{2+} indicator mouse model (Loggiacco et al., in press), *Csf1R-2A-GCaMP6m* to test for microglial

histamine responses in situ. In this mouse model, a transgenic *gcamp6m* cassette preceded by a 2A sequence is introduced right before the stop codon of the endogenous *Csf1r* gene, leading to the expression of the Ca^{2+} indicator protein GCaMP6m specifically in microglia. Acute cortical brain slices were generated from adult (P40-P90) male and female indicator mice to monitor microglial intracellular Ca^{2+} responses upon bath application of histamine (100 μM) using live-cell imaging (Figure 2a). In accordance to our observations in Loggiacco et al. (in press), the intensity of the GCaMP6m fluorescence under basal conditions was very low in this mouse model, and the fluorescence within microglia was nearly indistinguishable from background fluorescence. Microglial cells undergoing intracellular Ca^{2+} elevations, however, display strong enhancements in GCaMP6m fluorescence (see Figure 1a). Like in vitro experiments (see Figure 1),

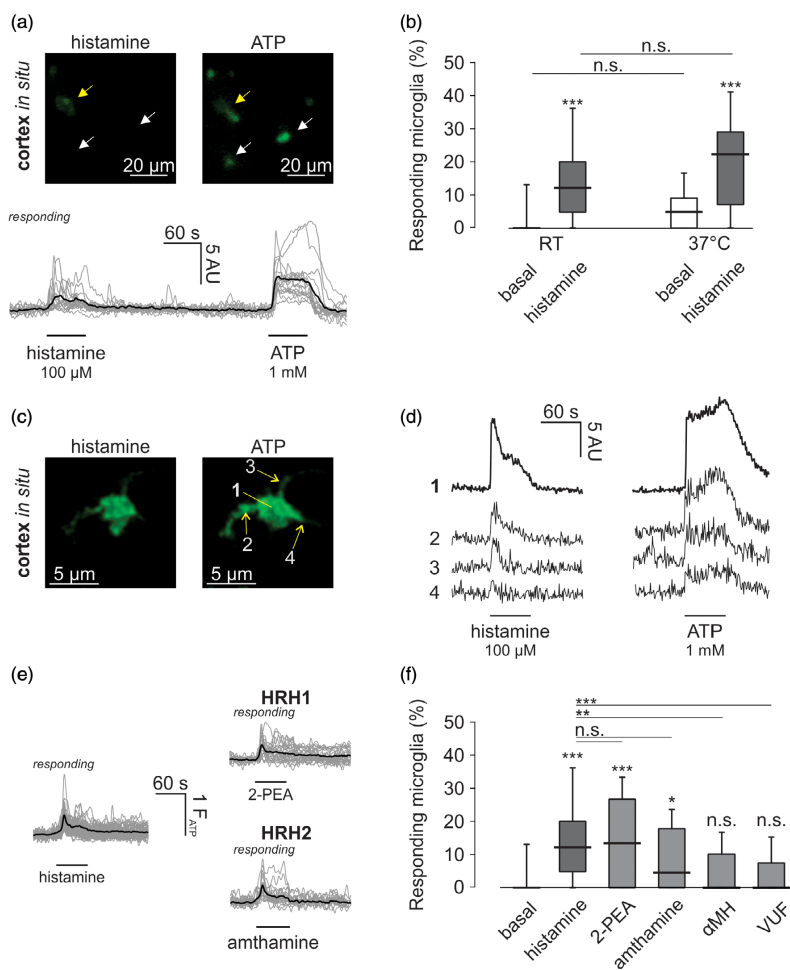


FIGURE 2 Cortical microglia in situ respond to histamine via *Hrh1* and *Hrh2*. (a) Top, representative microglial cells during live cell recordings from adult cortical brain slices in the presence of histamine (left) and ATP (right). Images were generated by subtraction of the movie frames before substance application from frames in the presence. Histamine-responding microglia are indicated with a yellow arrow, non-responding microglia with a white arrow. Bottom, overlay of intracellular Ca^{2+} responses to histamine from cortical microglia. The black trace is the average response of all responding cells (gray). (b) Summary of the percentage of histamine-responding microglia in situ (left). Average amplitudes of microglial histamine responses normalized to the amplitude of ATP responses (right). (c) Representative microglial cell during a 2-photon live-cell recording from an adult cortical brain slice in the presence of histamine (left) and ATP (right). Images were generated by subtraction of the movie frames before substance application from frames in the presence. Note that only proximal processes responded to ATP and histamine. (d) Intracellular Ca^{2+} responses from cortical histamine-responding microglia. Regions of interest of the traces are indicated by arrows in (c). (e) Overlay of intracellular Ca^{2+} responses from in situ cortical microglia responding to histamine, a *Hrh1*- (2-PEA, 100 μM) and a *Hrh2*- (Amthamine; 10 μM) specific agonist. Black traces indicate the average response of all responding cells (gray). (f) Summary of the percentage of responding microglia from experiments shown in (c), including those with *Hrh3*- (α -methylhistamine; 10 μM) and *Hrh4*- (VUF 10460; 10 μM) specific agonists. Box Plots indicate the median (black line) as well as the 25%–75% (box) and 10%–90% (whiskers) percentiles. Statistical significance was tested by a Kruskal Wallis test followed by Dunn's multiple comparisons test and is indicated as followed: n.s., $p \geq .05$; * $p \leq .05$; ** $p \leq .01$, *** $p \leq .001$. Number of mice/experiments/cells: N(basal) = 16/143/1296; N(histamine) = 11/45/747; N(2-PEA) = 4/24/167; N(amthamine) = 4/24/184; N(α MH) = 6/29/346; N(VUF) = 6/30/364; N(basal 37°C) = 4/19/261; N(histamine 37°C) = 4/21/272

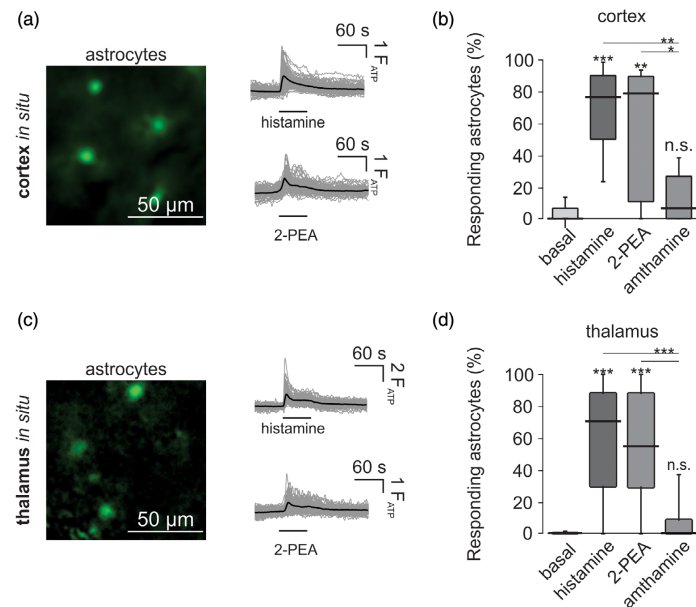


FIGURE 3 Astrocytes in cortex and thalamus respond to histamine via *Hrh1*. (a) Representative astrocytes from cortex during live cell imaging recordings from adult brain slices in the presence of the *Hrh1*-specific agonist 2-PEA. Slices were loaded with 10 μ M Fluo4/AM to record astrocytic Ca^{2+} level changes. Images were generated by subtraction of the movie frames before substance application from frames in the presence. Traces on the right show the overlay of intracellular Ca^{2+} responses from cortical histamine- or 2-PEA-responding astrocytes. Black traces indicate the average response of all responding cells (gray). (b) Summary of the percentage of histamine-, 2-PEA (*Hrh1* agonist)- and amthamine (*Hrh2* agonist)- responding astrocytes in cortical slices. (c) Same as (a) and (b) but data were obtained from in situ recordings in the thalamus. Box plots indicate the median (black line) as well as the 25%-75% (box) and 10%-90% (whiskers) percentiles. Statistical significance was tested by a Kruskal Wallis test followed by Dunn's multiple comparisons test and is indicated as followed: n.s., $p \geq .05$; *, $p \leq .05$; **, $p \leq .01$; ***, $p \leq .001$. Number of mice/experiments/cells: N(Cx basal) = 3/10/124; N(Cx histamine) = 4/11/143; N(Cx 2-PEA) = 3/10/124; N(Cx amthamine) = 3/11/129; N(Tha basal) = 4/47/457; N(Tha histamine) = 2/16/168; N(Tha 2-PEA) = 2/13/133; N(Tha amthamine) = 4/16/147

histamine in situ also induced Ca^{2+} elevations only in a subset of microglia (Figure 2b) with $12.1 \pm 5.3\%/20.0\%$ of ATP-responding cells being also responsive for histamine ($n = 747$ cells, 45 slices, 11 mice). The subpopulation of histamine-responding microglia was significantly larger in situ than in vitro ($p = .0105$). There were no significant differences between microglial responses from male and female brain slices ($p = .0657$). Histamine responses were often biphasic with a fast initial, transient rise and a second, sustained phase which reversed to baseline Ca^{2+} levels upon wash out of histamine (Figure 2a). The peak amplitude of the initial intracellular Ca^{2+} rise was on average $57.7 \pm 5.9\%$ of the ATP-evoked Ca^{2+} elevation. We also quantified the percentage of cells that responded randomly within a 60 s period before histamine application. $0.0 \pm 0.0/0.0\%$ of the ATP-responding microglia displayed this spontaneous activity indicating that histamine induced a significant response over baseline activity ($p < .0001$). There were no significant differences in basal ($p = .3226$) or histamine ($p > .9999$) responses when experiments were performed at 37°C

(Figure 2b). We next investigated if microglial histamine responses are also abundant in processes. As shown in Figure 2c,d, Ca^{2+} responses upon ATP application were, if at all, only found in the proximal parts of microglial processes. On average, 1.46 ± 0.31 (proximal) processes per microglia responded to ATP. We quantified the process Ca^{2+} signals upon histamine in microglia that displayed a somatic histamine response and found that the majority of ATP-responding processes (73.7%) did also respond to histamine. These data demonstrate that microglial Ca^{2+} responses to ATP and histamine are much more pronounced in somata than processes.

We next addressed the question if there is brain region-specific heterogeneity in microglial histamine responses and performed in situ live cell recordings in hippocampus, striatum, thalamus, and corpus callosum. As shown in Figure S2, microglia responded also in these brain regions upon application of 100 μ M histamine. The proportion of histamine-responding microglia was comparable to cortex in hippocampus ($7.3 \pm 0.0/20.0\%$; $n = 320$ cells, 46 slices, 10 mice; $p > .9999$),

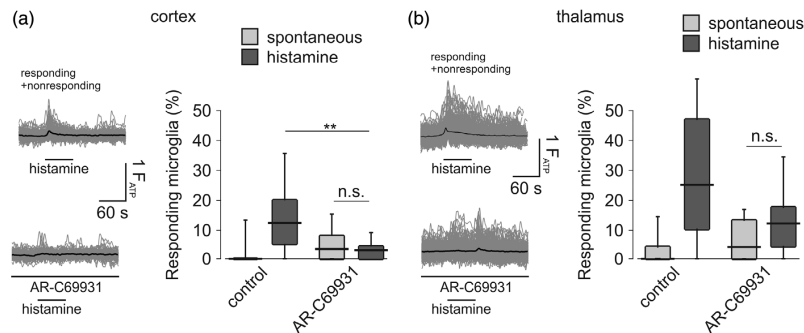


FIGURE 4 Histamine-evoked microglial Ca^{2+} responses depend on *P2ry12*. (a) Left, overlay of intracellular Ca^{2+} responses from in situ cortical microglia responding to histamine in the presence or absence of the *P2ry12* inhibitor AR-C69931 (1 μM). Black traces indicate the average response of all responding cells (gray). Note that unlike in the other figures, both responding and non-responding traces are shown in these plots. Right, summary of the percentage responding microglia from experiments shown in (a). (b) Same as (a) but data were obtained from thalamic microglia in situ. Box plots indicate the median (black line) as well as the 25%–75% (box) and 10%–90% (whiskers) percentiles. Statistical significance was tested by a Kruskal Wallis test followed by Dunn's multiple comparisons test and is indicated as followed: n.s., $p \geq .05$; *, $p \leq .05$; **, $p \leq .01$, *** $p \leq .001$. Number of mice/experiments/cells: N(Cx basal) = 16/143/1296; N(Cx histamine) = 11/45/747; N(Cx ARC basal) = 4/22/555; N(Cx ARC histamine) = 4/23/590; N(Tha basal) = 39/229/2250; N(Tha histamine) = 13/47/613; N(Tha ARC basal) = 4/20/393; N(Tha ARC histamine) = 4/16/147

striatum ($0.0 \pm 0.0/12.5\%$; $n = 238$ cells, 39 slices, 12 mice, $p = .0904$), thalamus ($25.0 \pm 11.9/45.8\%$; $n = 253$ cells, 37 slices, 12 mice; $p = .1611$) and corpus callosum ($22.5 \pm 5.8/52.1\%$; $n = 323$ cells, 36 slices, 12 mice; $p = .3635$). Significant differences were found between hippocampus and striatum in which microglia responded to a lesser extent to histamine than in thalamus ($p = .0023$ vs. HC; $p < .0001$ vs. Str) and in the corpus callosum ($p = .0105$ vs. HC; $p < .0001$ vs. Str).

Taken together, we conclude from these experiments that a sub-population of microglia responds to histamine in vitro and in situ, and that the percentage of histamine-responding microglia varied among different brain regions.

3.3 | Microglial histamine responses in situ are mediated by *Hrh1* and *Hrh2*

We next performed in situ Ca^{2+} recordings on cortical microglia using *Hrh* isoform-specific agonists (Figure 2c,d). Surprisingly, application of the *Hrh1*-specific agonist 2-pyridylethylamine dihydrochlorid (2-PEA; 100 μM) led to microglial Ca^{2+} elevations in $13.4 \pm 0.0/25.6\%$ of cortical microglia ($n = 184$ cells, 24 slices, 4 mice) which was not significantly different to the response rate upon 100 μM histamine ($p > .9999$). Amthamine (10 μM), which specifically activates *Hrh2* receptors, evoked also Ca^{2+} responses in $4.6 \pm 0.0/17.1\%$ of the microglia ($n = 184$ cells, 24 slices, 4 mice) which was still higher than spontaneous activity ($p = .0440$) and not different from histamine ($p = .4190$). The *Hrh3*- and *Hrh4*-specific agonists αMH (1 μM) and VUF 10460 (10 μM) did not evoke Ca^{2+} responses in cortical microglia.

We aimed at verifying these results in another brain region and investigated microglial Ca^{2+} responses upon *Hrh* isoform-specific agonists in the thalamus (see Figure S3). Like in the cortex, there was a significant portion of microglia ($18.2 \pm 9.6/34.1\%$; $n = 396$ cells, 43 slices, 6 mice) responding to the *Hrh1*-specific agonist 2-PEA (100 μM) which was similar to thalamic responses upon histamine ($p > .9999$; Figure S3A,B). The *Hrh2*-specific agonist amthamine also evoked Ca^{2+} responses in a subset of ATP-responding microglia ($13.4 \pm 8.3/19.6\%$; $n = 354$ cells, 34 slices, 6 mice; $p > .9999$). Isoform-specific activation of *Hrh3* ($0.0 \pm 0.0/5.4\%$; $n = 223$ cells, 34 slices, 6 mice) or *Hrh4* ($0.0 \pm 0.0/0.0\%$; $n = 275$ cells, 37 slices, 6 mice) did not have significant effects on microglial Ca^{2+} levels in thalamus when compared with spontaneous baseline activity. To further validate these results, we tested microglial histamine responses in thalamus in the presence of *Hrh*-isoform-specific blockers (Figure S3). Strikingly, the *Hrh1*-specific antagonist cetirizine (10 μM) significantly decreased microglial Ca^{2+} responses upon histamine application ($0.0 \pm 0.0/14.9\%$; $n = 244$ cells, 32 slices, 5 mice; $p < .0001$). Antagonizing *Hrh2* by using tiotidine (10 μM) did not significantly affect histamine responses of thalamic microglia ($15.5 \pm 7.9/26.7\%$; $n = 425$ cells from 38 slices and 6 mice; $p > .9999$). Likewise, *Hrh3* (carcinine; 10 μM) had no significant effects on microglial histamine responses ($18.33 \pm 0/34.37\%$; $n = 358$ cells, 40 slices, 6 mice; $p > .9999$; Figure S3A,B). Taken together, our data indicate the involvement of *Hrh1* and *Hrh2* in microglial histamine responses in cortex and thalamus, with *Hrh1* being more predominantly involved. These findings are in contrast to our data on isolated microglia demonstrating that *Hrh2* is the only microglia-intrinsic histamine receptor opening the possibility that the microglia *Hrh1*-mediated response could be indirect and mediated by another cell type.

3.4 | Hrh1-mediated microglial Ca²⁺ responses are indirectly mediated via astrocytes

Astrocytes express *Hrh1* receptors (Zhang et al., 2014) and were previously shown to respond with Ca²⁺ elevations to histamine via *Hrh1* (Jung et al., 2000). It suggests that they could be a potential source for signaling substances that are released in a histamine (*Hrh1*)-dependent fashion from astrocytes and sensed by microglia. We revisited the previous findings and studied astrocytic Ca²⁺ level changes in response to histamine in situ. AM-ester-coupled Ca²⁺ indicators are usually nicely taken up by cultured or isolated microglia (e.g., Elmadany, de Almeida Sassi, et al., 2020; Hoffmann et al., 2003; Moller et al., 2000), however, in brain slices taken up mainly by astrocytes (Schipke et al., 2002). We confirmed this previous finding by comparing Fluo4/AM labeling with fluorescence reporter expression in acute brain slices from GFAP-RFP mice. As shown in Figure S6, Fluo4/AM signals largely overlapped with RFP fluorescence (95.9 ± 3.9%), indicating that the Ca²⁺ indicator was taken up by GFAP⁺ cells, putatively astrocytes. In fact, this finding does not exclude non-astrocytic cell types with a similar morphology like NG2 cells. However, NG2 glia usually do not express GFAP (Dawson, 2003) and contribute to a rather low extent (2%–3%) to the cell population of the CNS as compared with GFAP⁺ astrocytes (10%–15%). We therefore conclude that the majority of the Fluo4-labelled cells in our slices are astrocytes and we used this Ca²⁺ indicator for loading cortical brain slices from C57/Bl6 mice. As shown in Figure 3a,b, 76.5 ± 52.5/87.9% of the cortical ATP-responding cells displayed Ca²⁺ elevations upon external application of 100 μM histamine (*n* = 143 cells, 11 slices, 3 mice) which was significantly more than basal, spontaneous astrocytic Ca²⁺ elevations (0.0 ± 0.0/6.4%; *p* = .0002). We did the same experiment in cortical slices from *Cs1r-2A-mCherry-2A-GCaMP* animals (Figure S7) and discriminated microglia by their transgenic mCherry fluorescence from astrocytes (mCherry⁻). The response rate of the mCherry⁺ cells was comparable to that of microglial cells in Figure 2 (12.5 ± 5.8/20.6%; *n* = 160 cells, 12 slices, 4 mice) and was significantly smaller than the response rate of mCherry⁻ cells (64.6 ± 42.6/88.8%; *n* = 158 cells, 14 slices, 4 mice).

The application of 2-PEA (*Hrh1* agonist; 100 μM) led to comparable astrocytic Ca²⁺ responses (80.0 ± 66.7/88.9%; *n* = 124 cells, 10 slices, 3 mice; *p* = .0013 vs. basal and *p* = .0013 vs. histamine), suggesting that *Hrh1* is the dominant histamine receptor isoform in cortical astrocytes. The astrocytic response rate upon the *Hrh2*-specific agonist amthamine was 6.5 ± 0.0/20.5% (*n* = 129 cells, 11 slices, 3 mice) which was not significantly different from basal activity (*p* > .9999). We also investigated thalamic astrocytes and found—similar to cortical astrocytes—the majority of cells responding to histamine (70.7 ± 32.1/82.7%; *n* = 168 cells, 16 slices, 2 mice; Figure 3c,d) and *Hrh1* stimulation (2-PEA; 60.0 ± 39.7/79.7%; *n* = 133 cells, 13 slices, 4 mice; *p* > .9999 vs. histamine) whereas there was no response upon *Hrh2* activation (amthamine; 0.0 ± 0.0/0.0%; *n* = 147 cells, 16 slices, 4 mice; *p* < .0001 vs. histamine).

We therefore conclude that astrocytes express functional *Hrh1* receptors in cortex and thalamus being, thus, potential sources of a *Hrh1*-dependent secondary signaling toward microglial receptors.

3.5 | Microglia Ca²⁺ responses to histamine are dependent on P2ry12 signaling

It has been previously shown that purinergic signaling is a strong communication pathway between astrocytes and microglia, and that astrocytic Ca²⁺ elevations can be followed by ATP release and subsequent microglial Ca²⁺ responses (Schipke et al., 2002; Verderio & Matteoli, 2001). The data above demonstrate that astrocytes but not microglia respond to *Hrh1* stimulation. In an attempt to test for the hypothesis that *Hrh1* stimulation indirectly mediates microglial Ca²⁺ responses via astrocytes and ATP release, we blocked P2ry12 which is specifically expressed by microglia in the brain, and which is the predominant (metabotropic) purinergic receptor in microglia (Figure 4a,b). Cortical brain slices from microglia Ca²⁺ indicator mice were incubated for 2 min with AR-C69931 (1 μM) prior to the application of histamine (100 μM). The blockade of P2ry12 dramatically reduced microglial histamine responses to levels indistinguishable from baseline activity: only 2.70 ± 0/3.72% of ATP-responding microglia displayed histamine responses in the presence of AR-C69931 (*n* = 590 cells, 23 slices, 4 mice; *p* = .6808 vs. basal and *p* = .0012 vs. histamine/control), suggesting that ATP is the messenger that causes cortical microglial Ca²⁺ responses upon histamine application. Microglia histamine responses were also inhibited in thalamus, however, to a lower extent. In the presence of AR-C69931, 12.0 ± 4.6/16.9% of the microglia responded upon histamine application (*n* = 393 cells from 20 slices and 4 mice). This was not significantly different from spontaneous activity (0.0 ± 0.0/1.1%, *p* = .6371), but there was also no significant differences to histamine application alone (25.0 ± 11.9/45.8%, *p* = .4579).

3.6 | Histamine stimulates microglial phagocytic activity via Hrh1

To study the effect of brain histamine on microglia at a more functional level, we tested if and how microglia phagocytosis is modulated by histamine. Phagocytic activity was quantified according to our previously published in situ assay (Wendt et al., 2017). Acute brain slices from adult C57BL/6J mice were incubated for 60 min with latex beads and the number of beads incorporated into a 3D-rendered Iba1-labeled (microglia) volume was subsequently counted using confocal imaging and 3D reconstruction (Figure 5a). Per animal and condition, we quantified microglial phagocytosis in 4–5 cortical brain slices, analyzing 4–5 randomly chosen fields of view per slice by z-stacks in the cortex (layers I–VI). As shown in Figure 5b, baseline phagocytic index in the cortex (1.65 ± 0.93/2.47; *n* = 54) was significantly enhanced when histamine (100 μM) was co-applied together with the beads (2.87 ± 2.14/3.87; *n* = 90; *p* < .0001). As there was only a low percentage of cortical microglia responding to histamine with intracellular Ca²⁺ elevations (12.1 ± 5.3%/20.0%; see Figure 2a,b), we addressed the question if the increase in microglial phagocytosis upon histamine incubation could be due to a stimulation of only a subpopulation of microglial cells (Figure S4A), and therefore determined the

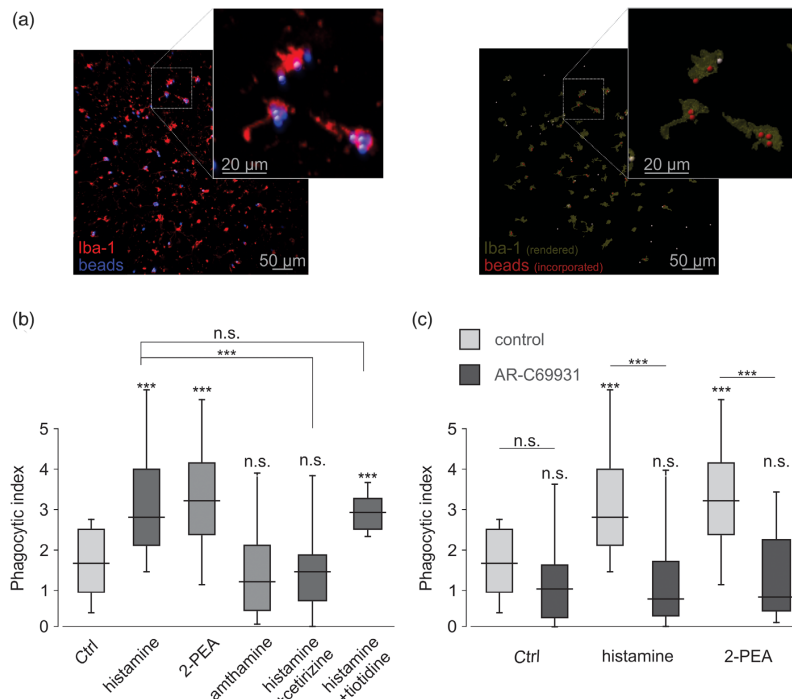


FIGURE 5 Microglial phagocytosis in the cortex is stimulated by histamine via *Hrh1* and *P2ry12*. (a) *Left*, representative confocal image of Iba1-stained cortical microglia (red) together with latex beads (blue) performed on brain slices from an adult WT male mouse. *Right*, 3D reconstruction of Iba1-positive microglia is shown with automatically counted phagocytosed beads (shown in red). Scale bars: 50 μ m. The insert shows the cells at higher magnification. (b) Comparison of phagocytic activity of cortical microglia under control conditions (white), in the presence of histamine (black), in the presence of the subtype-specific histamine receptor agonists 2-PEA (*Hrh1* agonist; 100 μ M gray) or amthamine (*Hrh2* agonist; 10 μ M; gray) or in the presence of histamine plus the subtype-specific histamine receptor antagonists cetirizine (*Hrh1* antagonist; 10 μ M; black) or tiotidine (*Hrh2* antagonist; 10 μ M; black). Phagocytic index indicates the number of incorporated beads per Iba⁺ volume (see material and methods). (c) Effect of *P2ry12* blockade (1 μ M AR-C69931) on microglial phagocytic activity under control and under histamine (100 μ M)- or 2-PEA (100 μ M)-stimulating conditions. Box plots indicate the median (black line) as well as the 25%–75% (box) and 10%–90% (whiskers) percentiles. Statistical significance was tested by a Kruskal Wallis test followed by Dunn's multiple comparisons test and is indicated as follows: n.s., $p \geq .05$; * $p \leq .05$; ** $p \leq .01$; *** $p \leq .001$. Number of mice/slices: N(Ctrl) = 6/55; N(histamine) = 6/90; N(2-PEA) = 3/34; N(amthamine) = 3/33; N(histamine+cetirizine) = 3/44; N(histamine+tiotidine) = 2/20; N(ARC) = 3/45; N(histamine+ARC) = 3/45; N(2-PEA+ARC) = 3/45

fraction of phagocytosing microglia under control and histamine-stimulating conditions. Under control conditions, on average 6.7 ± 0.6 microglial cells per view field incorporated one bead, which increased to 12.3 ± 0.7 cells during histamine incubation ($p < .0001$, Figure S4A). Comparing microglial cells incorporating two or more beads under control and histamine-stimulating conditions led to a similar increase (2 beads: 1.6 ± 0.3 and 4.4 ± 0.4 microglia/VF; 3 beads: 0.5 ± 0.1 and 1.6 ± 0.2 microglia/VF; 4 beads: 0.1 ± 0.1 and 0.7 ± 0.1 microglia/VF for control and histamine, respectively; $p < .0001$ for all comparisons). As the total number of microglial cells within each

scanned volume ($225 \mu\text{m} \times 225 \mu\text{m} \times 21 \mu\text{m}$) was 113.3 ± 4.4 ($n = 144$ view fields), the histamine-induced increase in phagocytosis was apparent in $9.2 \pm 0.4\%$ of the observed microglia which is in a similar range like histamine-responding microglia in Ca^{2+} imaging experiments.

Microglia Ca^{2+} responses to histamine have been similar in thalamus and cortex (see Figure S2B). We therefore tested if the stimulation of phagocytic activity by histamine is also comparable in thalamus. Interestingly, thalamic microglial phagocytosis was generally at a lower level than cortical, with a phagocytic index of 0.44

$\pm 0.15/0.59$ under control conditions ($n = 36$; $p < .0001$ vs. cortex, Figure S5). As in the cortex, a significant stimulation of phagocytosis occurred in the presence of histamine ($1.11 \pm 0.63/1.42$; $n = 33$; $p < .0001$ vs. ctrl). The increase in phagocytosing microglia was $11.5 \pm 2.0\%$, and not significantly different from cortex ($p = .5863$).

In an attempt to further study the histamine-induced stimulation of microglial phagocytosis, we also tested the isoform-specific agonists 2-PEA (100 μM ; *Hrh1*), amthamine (10 μM ; *Hrh2*), R-(−)- α -methylhistamine dihydrobromide (αMH ; 1 μM ; *Hrh3*), or VUF 10460 (10 μM ; *Hrh4*) in order to activate histamine receptors in a subtype-specific manner. Interestingly, as summarized in Figure 5b, only incubation with the *Hrh1*-specific agonist 2-PEA elevated microglial phagocytosis in cortex ($3.24 \pm 2.38/3.77$; $n = 34$; $p < .0001$ and $p > .9999$ compared with control and histamine, respectively) whereas there was no effect when *Hrh2* were specifically activated ($1.25 \pm 0.48/1.93$; $n = 33$; $p > .9999$ vs. control, Figure 5b). There was likewise no effect on phagocytosis by stimulation of *Hrh3* ($1.67 \pm 0.58/2.01$; $n = 28$; $p < .8299$ vs. control, data not shown) or *Hrh4* ($1.86 \pm 1.41/2.26$; $n = 15$; $p > .9999$ vs. control, data not shown). We further verified these results by blocking *Hrh1* receptors using Cetirizine dihydrochloride (5 μM) when slices were incubated with histamine. Indeed, histamine-mediated stimulation of phagocytosis was completely blocked by *Hrh1* inhibition ($1.45 \pm 0.73/1.81$; $n = 44$; $p > .9999$ vs. control). The blockade of *Hrh2* by using 10 μM tiotidine did not affect cortical phagocytosis of microglia.

In thalamus, the *Hrh* subtype-specific effects on microglia phagocytic activity were similar to cortex (Figure S5B), with a stimulation by 2-PEA (*Hrh1*) that was comparable to histamine and no effects of amthamine (*Hrh2*). Furthermore, only *Hrh1*, but not *Hrh2*, inhibition prevented histamine-induced stimulation of microglial phagocytosis. Taken together, our data demonstrate that histamine stimulates microglial phagocytosis via *Hrh1*, but not by *Hrh2* activation in cortex and thalamus. Similar to acute intracellular Ca^{2+} elevations upon histamine application, histamine incubation for 1 h increased the phagocytic activity also only in a subset of microglial cells.

3.7 | Stimulation of microglial phagocytic activity by histamine is dependent on P2ry12

We finally tested if the *Hrh1*-dependent, histamine-evoked stimulation of microglial phagocytosis is dependent on putatively secondary purinergic signals. AR-C69931 was used to block microglial P2ry12 receptors during the 1 h incubation with the beads. As shown in Figure 5c, AR-C69931 indeed completely inhibited histamine-stimulated phagocytosis in cortex. The phagocytic index in the presence of histamine together with AR-C69931 was $0.7 \pm 0.28/1.61$ ($n = 45$) and therefore significantly lower than with histamine alone ($2.87 \pm 2.14/3.99$; $n = 90$; $p < .0001$) as well as similar to baseline phagocytic activity under control conditions ($1.65 \pm 0.92/2.51$; $n = 54$; $p = .3631$) or in the presence of AR-C69931 alone ($0.98 \pm 0.29/1.56$; $n = 54$; $p > .9999$). Similarly, the stimulating effect of the *Hrh1*-specific agonist 2-PEA (100 μM ; $3.24 \pm 2.35/4.06$) was

completely abolished by AR-C69931 ($0.75 \pm 0.43/1.92$; $n = 45$; $p < .0001$ vs. 2-PEA alone). In thalamus, the *Hrh1*-dependent stimulation of microglia phagocytosis was also abolished by AR-C69931 (Figure S5). In the presence of the P2ry12 blocker, histamine ($0.18 \pm 0.07/0.44$; $n = 36$) did not potentiate microglia phagocytic activity, suggesting that the cellular and molecular mechanisms of the stimulation are not different from cortex. Taken together, our data suggest that histamine-evoked stimulation of microglial phagocytosis depends on microglial P2ry12 receptors in cortex and thalamus.

4 | DISCUSSION

Tonic brain histamine levels are controlled by histaminergic neurons in the tuberomammillary nucleus (TMN) in a circadian fashion and have an impact on various brain pathologies. In the present study, we investigated which receptors and pathways are involved in microglial histamine responses. In freshly isolated microglia, only the *Hrh2*-specific agonist amthamine did evoke intracellular Ca^{2+} elevations while agonists of other subtypes of histaminergic receptors did not trigger responses. Furthermore, only the blockade of *Hrh2* but not of the other *Hrh* isoforms did inhibit histamine responses of isolated microglia. We therefore confirmed many previous transcriptomic observations that microglia express *Hrh2* and not histaminergic receptors of the other three subtypes on a functional level (Butovsky et al., 2014; Consortium, 2018; Grabert et al., 2016; Hickman et al., 2013; Zhang et al., 2014).

In a tissue context, namely in cortical and thalamic brain slices, the *Hrh2*-specific agonist amthamine did trigger a response, but we found also responses upon *Hrh1* activation which were even more prominent. The transcriptomic data indicate that *Hrh1* receptors are functionally expressed by the majority of astrocytes but not in microglia. The sensitivity of microglial *Hrh1* responses to the P2ry12 inhibitor AR-C69931 strongly suggests an astrocyte to microglia communication via ATP/ADP and P2ry12. We assume that activation of *Hrh1* receptors in astrocytes triggers the release of ATP/ADP which stimulates intracellular Ca^{2+} elevations and phagocytic activity in microglia via activation of P2ry12 purinergic receptors. It is well established that these receptors are prominently expressed by microglia and that activation of these receptors can stimulate phagocytosis (Elmadany, Loggiacco, et al., 2020; Inoue et al., 2009; Koizumi et al., 2007). In a recent study, we found even a significant decrease in microglia phagocytic activity in the cortex of P91-P112 male and female WT mice when P2ry12 was blocked. The reason why this result could not be confirmed in the current study might be due to the different age of the mice which was only P30–P60 here. A systematic approach of this interesting issue still remains elusive.

The treatment of acute brain slices with amthamine did not affect microglial phagocytic activity, suggesting that there is only little involvement of microglia-intrinsic *Hrh2* in controlling phagocytic activity. One possible biological role for microglial *Hrh2* receptors could be that *Hrh2* expression is low and negligible under healthy conditions, but that microglia become more directly sensitive to histamine under



disease conditions as suggested by results from a previous publication of our lab in which LPS treatment significantly increased microglia responses to histamine in adult cultures (Pannell et al., 2014). Another possibility would be that *Hrh2* affects other microglial properties than phagocytosis, that is, the ramification (Frick et al., 2016), or that we oversaw potential microglia histamine responses that do not affect intracellular Ca^{2+} levels (e.g., cAMP). We could also consider that histamine receptors are not evenly distributed among the surface of microglia and that *Hrh2* receptors are located rather in microglial processes than in the soma. Our Ca^{2+} responses are, however, dominated by signals from soma. *Hrh2* (and also *P2ry12*) receptors are known to be linked to cAMP signaling pathways, and not-like *Hrh1* - to Ca^{2+} . However, it has been previously observed that GPCRs linked to G_i or G_s proteins can also elicit intracellular Ca^{2+} elevations (Elmadany, de Almeida Sassi, et al., 2020; Kuhn et al., 2004; Pannell et al., 2014), potentially by signaling of the $G\beta\gamma$ subunits in a PLC/IP₃R-dependent fashion from internal stores (Clapham, 2007). Ca^{2+} elevations downstream of *Hrh2* (Esbenshade et al., 2003) or *P2ry12* (De Simone et al., 2010; Irino et al., 2008; Jiang et al., 2017; Pausch et al., 2004) activation were previously demonstrated. We therefore suggest that microglial *Hrh2*- and *P2ry12*-dependent Ca^{2+} responses in the current study also originate from internal release. This hypothesis would fit to our data about the sparse responses to ATP or histamine in microglial thin processes which are probably not equipped with endoplasmic reticulum or other Ca^{2+} stores.

The ambient, average histamine concentration in the extracellular space of the brain is considered to be in the range of 0.5 to 2 μ M (Best et al., 2017). That does not exclude that it can be significantly higher in micro-compartments and has indeed been shown to locally increase up to 20-fold under pathophysiological conditions (Haas & Panula, 2003; Panula & Nuutinen, 2013). We used in the present study a histamine concentration of 100 μ M not to mimic physiological HA level changes but rather to test for the presence of functional *Hrh* isoforms on microglia and astrocytes. The physiological relevance of our data are, thus, more on the functional expression of *Hrh* isoforms and downstream cellular pathways. In the current study, we used acute brain slices from healthy, young adult mice. Previous *in vivo* data have shown that calcium signaling in microglia depends on brain state, the inflammatory status and the activity of surrounding neurons (Brawek & Garaschuk, 2013; Eichhoff et al., 2011; Umpierre et al., 2020; Umpierre & Wu, 2020). Although we did not investigate microglia histamine responses *in vivo*, it seems very unlikely that the involvement of astrocytic *Hrh1* and microglial *P2ry12* is different in the living brain. Furthermore, there could be alterations under disease conditions due to pathophysiological changes in *Hrh* or *P2ry12* receptor expression levels or altered levels of ambient histamine.

In the current study we neither demonstrated nor ruled out a functional role of microglial Ca^{2+} signaling in phagocytosis. However, stimulation of *Hrh1* which is functionally expressed on astrocytes, stimulated microglial phagocytosis in a (microglial) *P2ry12*-dependent fashion. Our data therefore indicate that astrocytes are required for histamine stimulation of microglial phagocytic activity. There are several previous reports on the impact of histamine on microglia

phagocytosis; however, there is so far no evidence for a potential interaction of astrocytes in microglial responses. In fact, studies on acutely isolated or cultured microglial cells, including the relatively non-physiological cell line N9, do not contain other cell types like astrocytes as potential source of secondary messengers (Albertini et al., 2020; Barata-Antunes et al., 2017; Ferreira et al., 2012; Iida et al., 2015; Rocha et al., 2016). To the best knowledge of the authors, there are so far two studies testing the effect of histamine on microglial phagocytosis under more physiological *in situ* or *in vivo* conditions. One study showed that microglia phagocytosis was suppressed by inhibition of *Hrh3* in organotypic hippocampal brain slices. The *in vivo* injection of the inverse *Hrh3* agonist JNJ10181457 into the prefrontal cortex, however, did only affect the LPS stimulation of microglia phagocytic activity, but had no effect on unstimulated microglia (Iida et al., 2017). As we did in the present study not directly test for these conditions and brain regions, these data do not necessarily contradict our results and it is quite tempting to speculate about the differences to our results. Conceivable explanations for the involvement of *Hrh3* in Iida et al. (2017) might for instance be the high density of neurons in the pyramidal layers of the hippocampus. Given that *Hrh3* is mainly expressed by neurons, it seems possible that blockade of *Hrh3* could rather have inhibited a yet unknown neuron-microglia communication than acting on microglia directly. In the present study, by using *in situ* Ca^{2+} imaging, we did not find any evidence for functional *Hrh3* expression on cortical and thalamic microglia and the transcriptomic data do also not support that hypothesis (Figures 1d, 2d and S3C,D). In Iida et al., however, the activation of microglia in the prefrontal cortex by LPS will have changed their expression profile, which potentially lead to an upregulation of microglia-intrinsic *Hrh3*. The second *in vivo* study on histamine and microglia phagocytosis was performed by Rocha et al. (2016) who found that stereotactical co-injection of histamine increased microglial engulfment of phosphatidylcholine-containing liposomes in the substantia nigra, according to a stimulation of microglial phagocytic activity by histamine. This result fits well to our findings, although the interplay between histamine and astrocytes was not tested directly. It was actually demonstrated in the same study that histamine did also stimulate phagocytosis of N9 microglia cultures in a *Hrh1*-dependent fashion however, the comparability of N9 microglia cultures and microglia *in situ* or *in vivo* is rather poor (Butovsky et al., 2014).

A further finding of the present study is that there are significant differences in microglial responses to histamine between different brain regions. Interestingly, microglia responses increased in corpus callosum and thalamus, thus, brain regions with a larger percentage of white matter. In thalamus, there was a similar *Hrh* subtype-specific activation pattern as in the cortex, suggesting that not the microglia-intrinsic expression of *Hrh* isoforms but rather the microglia communication with non-microglial cells could vary between different brain regions.

Histamine acts as a modulatory neurotransmitter and is linked to the maintenance of wakefulness in the healthy brain. Abnormalities in the histaminergic system have been associated with many brain diseases like Parkinson's disease or multiple sclerosis (Panula & Nuutinen, 2013). Microglia contribute to many physiological and

nearby all pathological processes in the CNS, and their ability to sense histaminergic tones or stimuli via astrocytes and P2ry12 might have an important impact on their behavior, including phagocytosis or synaptic pruning. We therefore conclude that all histamine-related processes in the brain could be potentially linked to microglial action via purinergic pathways, and this unexpected connection might be essential for the future development of novel immune-related therapies.

ACKNOWLEDGMENTS

We thank Regina Piske, Nadine Scharek, Bastiaan Pierik, and the microscopy core facility (Advanced Light Microscopy, ALM) of the MDC Berlin for technical assistance. We also thank Dr. Ralf Kühn and Andrea Leschke from the Transgenic Core Facility of the MDC for generating the microglia indicator mouse lines. This work was supported by the Helmholtz-Gemeinschaft, Zukunftsthema "Immunology and Inflammation" (ZT-0027), and by the Einstein-Stiftung. Open Access funding enabled and organized by Projekt DEAL.

CONFLICT OF INTEREST

The authors declare that they have no conflicts of interest with the contents of the article.

DATA AVAILABILITY STATEMENT

Data tables will be shared.

ORCID

Pengfei Xia  <https://orcid.org/0000-0001-5086-1755>

Helmut Kettenmann  <https://orcid.org/0000-0001-8208-0291>

REFERENCES

- Albertini, G., Etienne, F., & Roumier, A. (2020). Regulation of microglia by neuromodulators: Modulations in major and minor modes. *Neuroscience Letters*, 733, 135000. <https://doi.org/10.1016/j.neulet.2020.135000>
- Apolloni, S., Fabbrizio, P., Amadio, S., Napoli, G., Verdile, V., Morello, G., ... Volonté, C. (2017). Histamine regulates the inflammatory profile of SOD1-G93A microglia and the histaminergic system is dysregulated in amyotrophic lateral sclerosis. *Frontiers in Immunology*, 8, 1689. <https://doi.org/10.3389/fimmu.2017.01689>
- Bader, M. F., Taupenot, L., Ulrich, G., Aunis, D., & Ciesielski-Treska, J. (1994). Bacterial endotoxin induces $[Ca^{2+}]_i$ transients and changes the organization of Actin in microglia. *Glia*, 11(4), 336–344.
- Barata-Antunes, S., Cristóvão, A. C., Pires, J., Rocha, S. M., & Bernardino, L. (2017). Dual role of histamine on microglia-induced neurodegeneration. *Biochimica et Biophysica Acta - Molecular Basis of Disease*, 1863(3), 764–769. <https://doi.org/10.1016/j.bbdis.2016.12.016>
- Best, J., Nijhout, H. F., Samaranyake, S., Hashemi, P., & Reed, M. (2017). A mathematical model for histamine synthesis, release, and control in varicosities. *Theoretical Biology & Medical Modelling*, 14(1), 24. <https://doi.org/10.1186/s12976-017-0070-9>
- Boucsein, C., Zacharias, R., Farber, K., Pavlovic, S., Hanisch, U. K., & Kettenmann, H. (2003). Purinergic receptors on microglial cells: Functional expression in acute brain slices and modulation of microglial activation in vitro. *The European Journal of Neuroscience*, 17(11), 2267–2276.
- Bowman, R. L., Klemm, F., Akkari, L., Pyonteck, S. M., Sevenich, L., Quail, D. F., ... Joyce, J. A. (2016). Macrophage ontogeny underlies differences in tumor-specific education in brain malignancies. *Cell Reports*, 17(9), 2445–2459. <https://doi.org/10.1016/j.celrep.2016.10.052>
- Brawek, B., & Garaschuk, O. (2013). Microglial calcium signaling in the adult, aged and diseased brain. *Cell Calcium*, 53(3), 159–169. <https://doi.org/10.1016/j.ceca.2012.12.003>
- Butovsky, O., Jedrychowski, M. P., Moore, C. S., Cialic, R., Lanser, A. J., Gabriely, G., ... Weiner, H. L. (2014). Identification of a unique TGF-beta-dependent molecular and functional signature in microglia. *Nature Neuroscience*, 17(1), 131–143. <https://doi.org/10.1038/nn.3599>
- Clapham, D. E. (2007). Calcium Signaling. *Cell*, 131(6), 1047–1058. <https://doi.org/10.1016/j.cell.2007.11.028>
- Dawson, M. R., Polito, A., Levine, J. M., & Reynolds, R. (2003). NG2-expressing glial progenitor cells: an abundant and widespread population of cycling cells in the adult rat CNS. *Molecular and Cellular Neuroscience*, 24(2), 476–488. [https://doi.org/10.1016/s1044-7431\(03\)00210-0](https://doi.org/10.1016/s1044-7431(03)00210-0)
- De Simone, R., Niturad, C. E., De Nuccio, C., Ajmone-Cat, M. A., Visentin, S., & Minghetti, L. (2010). TGF-beta and LPS modulate ADP-induced migration of microglial cells through P2Y1 and P2Y12 receptor expression. *Journal of Neurochemistry*, 115(2), 450–459. <https://doi.org/10.1111/j.1471-4159.2010.06937.x>
- Eichhoff, G., Brawek, B., & Garaschuk, O. (2011). Microglial calcium signal acts as a rapid sensor of single neuron damage in vivo. *Biochimica et Biophysica Acta*, 1813(5), 1014–1024. <https://doi.org/10.1016/j.bbmr.2010.10.018>
- Elmadany, N., de Almeida Sassi, F., Wendt, S., Logiaco, F., Visser, J., Haage, V., ... Semtner, M. (2020). The VGF-derived peptide TLQP21 impairs purinergic control of chemotaxis and phagocytosis in mouse microglia. *The Journal of Neuroscience*, 40(17), 3320–3331. <https://doi.org/10.1523/jneurosci.1458-19.2020>
- Elmadany, N., Logiaco, F., Buonfiglioli, A., Haage, V. C., Wright-Jin, E. C., Schattenberg, A., ... Gutmann, D. H. (2020). Neurofibromatosis 1 - mutant microglia exhibit sexually-dimorphic cyclic AMP-dependent purinergic defects. *Neurobiology of Disease*, 144, 105030. <https://doi.org/10.1016/j.nbd.2020.105030>
- Esbenshade, T. A., Hee Kang, C., Krueger, K. M., Miller, T. R., Witte, D. G., Roch, J. M., ... Hancock, A. A. (2003). Differential activation of dual signaling responses by human H1 and H2 histamine receptors. *Journal of Receptor and Signal Transduction Research*, 23(1), 17–31. <https://doi.org/10.1081/rrs-120018758>
- Ferreira, R., Santos, T., Gonçalves, J., Baltazar, G., Ferreira, L., Agasse, F., & Bernardino, L. (2012). Histamine modulates microglia function. *Journal of Neuroinflammation*, 9, 90. <https://doi.org/10.1186/1742-2094-9-90>
- Frick, L., Rapanelli, M., Abbasi, E., Ohtsu, H., & Pittenger, C. (2016). Histamine regulation of microglia: Gene-environment interaction in the regulation of central nervous system inflammation. *Brain, Behavior, and Immunity*, 57, 326–337. <https://doi.org/10.1016/j.bbi.2016.07.002>
- Grabert, K., Michoel, T., Karavolos, M. H., Clohisey, S., Baillie, J. K., Stevens, M. P., ... McColl, B. W. (2016). Microglial brain region-dependent diversity and selective regional sensitivities to aging. *Nature Neuroscience*, 19(3), 504–516. <https://doi.org/10.1038/nn.4222>
- Haas, H., & Panula, P. (2003). The role of histamine and the tuberomammillary nucleus in the nervous system. *Nature Reviews. Neuroscience*, 4(2), 121–130. <https://doi.org/10.1038/nrn1034>
- Hickman, S. E., Kingery, N. D., Ohsumi, T. K., Borowsky, M. L., Wang, L. C., Means, T. K., & El Khoury, J. (2013). The microglial sensome revealed by direct RNA sequencing. *Nature Neuroscience*, 16(12), 1896–1905. <https://doi.org/10.1038/nn.3554>
- Hirrlinger, P. G., Scheller, A., Braun, C., Quintela-Schneider, M., Fuss, B., Hirrlinger, J., & Kirchhoff, F. (2005). Expression of reef coral fluorescent proteins in the central nervous system of transgenic mice. *Molecular and Cellular Neuroscience*, 30(3), 291–303. <https://doi.org/10.1016/j.mcn.2005.08.011>
- Hoffmann, A., Kann, O., Ohlemeyer, C., Hanisch, U. K., & Kettenmann, H. (2003). Elevation of basal intracellular calcium as a central element in the activation of brain macrophages (microglia): Suppression of



- receptor-evoked calcium signaling and control of release function. *The Journal of Neuroscience*, 23(11), 4410–4419.
- Iida, T., Yoshikawa, T., Kárpáti, A., Matsuzawa, T., Kitano, H., Mogi, A., ... Yanai, K. (2017). JNJ10181457, a histamine H3 receptor inverse agonist, regulates in vivo microglial functions and improves depression-like behaviours in mice. *Biochemical and Biophysical Research Communications*, 488(3), 534–540. <https://doi.org/10.1016/j.bbrc.2017.05.081>
- Iida, T., Yoshikawa, T., Matsuzawa, T., Naganuma, F., Nakamura, T., Miura, Y., ... Yanai, K. (2015). Histamine H3 receptor in primary mouse microglia inhibits chemotaxis, phagocytosis, and cytokine secretion. *Glia*, 63(7), 1213–1225. <https://doi.org/10.1002/glia.22812>
- Inoue, K., Koizumi, S., Kataoka, A., Tozaki-Saitoh, H., & Tsuda, M. (2009). P2Y₆-evoked microglial phagocytosis. *International Review of Neurobiology*, 85, 159–163.
- Irino, Y., Nakamura, Y., Inoue, K., Kohsaka, S., & Ohsawa, K. (2008). Akt activation is involved in P2Y₁₂ receptor-mediated chemotaxis of microglia. *Journal of Neuroscience Research*, 86(7), 1511–1519.
- Jiang, P., Xing, F., Guo, B., Yang, J., Li, Z., Wei, W., ... Xu, J. (2017). Nucleotide transmitters ATP and ADP mediate intercellular calcium wave communication via P2Y_{12/13} receptors among BV-2 microglia. *PLoS One*, 12(8), e0183114. <https://doi.org/10.1371/journal.pone.0183114>
- Jung, S., Pfeiffer, F., & Deitmer, J. W. (2000). Histamine-induced calcium entry in rat cerebellar astrocytes: Evidence for capacitative and non-capacitative mechanisms. *The Journal of Physiology*, 3, 549–561. <https://doi.org/10.1111/j.1469-7793.2000.00549.x>
- Juric, D. M., Kržan, M., & Lipnik-Stangelj, M. (2016). Histamine and astrocyte function. *Pharmacological Research*, 111, 774–783. <https://doi.org/10.1016/j.phrs.2016.07.035>
- Kettenmann, H., Hanisch, U. K., Noda, M., & Verkhratsky, A. (2011). Physiology of microglia. *Physiological Reviews*, 91(2), 461–553. <https://doi.org/10.1152/physrev.00011.2010>
- Koizumi, S., Shigemoto-Mogami, Y., Nasu-Tada, K., Shinozaki, Y., Ohsawa, K., Tsuda, M., ... Inoue, K. (2007). UDP acting at P2Y₆ receptors is a mediator of microglial phagocytosis. *Nature*, 446(7139), 1091–1095. <https://doi.org/10.1038/nature05704>
- Korvers, L., de Andrade Costa, A., Mersch, M., Matyash, V., Kettenmann, H., & Sementner, M. (2016). Spontaneous Ca²⁺ transients in mouse microglia. *Cell Calcium*, 60(6), 396–406. <https://doi.org/10.1016/j.ceca.2016.09.004>
- Kuhn, S. A., van Landeghem, F. K., Zacharias, R., Färber, K., Rappert, A., Pavlovic, S., ... Kettenmann, H. (2004). Microglia express GABA(B) receptors to modulate interleukin release. *Molecular and Cellular Neurosciences*, 25(2), 312–322. <https://doi.org/10.1016/j.mcn.2003.10.023>
- Logiaco, F., Xia, P., Georgiev, S., Chang, Y.-J., Franconi, C., Ugursu, B., Wolf, S., Kühn, R., Kettenmann, H., & Sementner, M. (in press). Microglial cells sense neuronal activity indirectly via astrocyte GABA release in the postnatal hippocampus. *Cell Reports*.
- Moller, T., Kann, O., Verkhratsky, A., & Kettenmann, H. (2000). Activation of mouse microglial cells affects P2 receptor signaling. *Brain Research*, 853(1), 49–59.
- Nikodemova, M., & Watters, J. J. (2012). Efficient isolation of live microglia with preserved phenotypes from adult mouse brain. *Journal of Neuroinflammation*, 9, 147. <https://doi.org/10.1186/1742-2094-9-147>
- Pannell, M., Szulzewsky, F., Matyash, V., Wolf, S. A., & Kettenmann, H. (2014). The subpopulation of microglia sensitive to neurotransmitters/neurohormones is modulated by stimulation with LPS, interferon-gamma, and IL-4. *Glia*, 62(5), 667–679. <https://doi.org/10.1002/glia.22633>
- Panula, P., & Nuutinen, S. (2013). The histaminergic network in the brain: Basic organization and role in disease. *Nature Reviews. Neuroscience*, 14(7), 472–487. <https://doi.org/10.1038/nrn3526>
- Passani, M. B., Bacciottini, L., Mannaioni, P. F., & Blandina, P. (2000). Central histaminergic system and cognition. *Neuroscience and Biobehavioral Reviews*, 24(1), 107–113.
- Pausch, M. H., Lai, M., Tseng, E., Paulsen, J., Bates, B., & Kwak, S. (2004). Functional expression of human and mouse P2Y₁₂ receptors in *Saccharomyces cerevisiae*. *Biochemical and Biophysical Research Communications*, 324(1), 171–177. <https://doi.org/10.1016/j.bbrc.2004.09.034>
- Rocha, S. M., Saraiva, T., Cristóvão, A. C., Ferreira, R., Santos, T., Esteves, M., ... Bernardino, L. (2016). Histamine induces microglia activation and dopaminergic neuronal toxicity via H1 receptor activation. *Journal of Neuroinflammation*, 13(1), 137. <https://doi.org/10.1186/s12974-016-0600-0>
- Sala Frigerio, C., Wolfs, L., Fattorelli, N., Thrupp, N., Voytyuk, I., Schmidt, I., ... de Strooper, B. (2019). The major risk factors for Alzheimer's disease: Age, sex, and genes modulate the microglia response to Aβ plaques. *Cell Reports*, 27(4), 1293–1306.e6. <https://doi.org/10.1016/j.celrep.2019.03.099>
- Schipke, C. G., Boucsein, C., Ohlemeyer, C., Kirchhoff, F., & Kettenmann, H. (2002). Astrocyte Ca²⁺ waves trigger responses in microglial cells in brain slices. *The FASEB Journal*, 16(2), 255–257. <https://doi.org/10.1096/fj.01-0514fj>
- Tabula Muris Consortium, T. M. (2018). Single-cell transcriptomics of 20 mouse organs creates a Tabula Muris. *Nature*, 562(7727), 367–372. <https://doi.org/10.1038/s41586-018-0590-4>
- Thangam, E. B., Jemima, E. A., Singh, H., Baig, M. S., Khan, M., Mathias, C. B., ... Saluja, R. (2018). The role of histamine and histamine receptors in mast cell-mediated allergy and inflammation: The hunt for new therapeutic targets. *Frontiers in Immunology*, 9(1873). <https://doi.org/10.3389/fimmu.2018.01873>
- Umpierre, A. D., Bystrom, L. L., Ying, Y., Liu, Y. U., Worrell, G., & Wu, L. J. (2020). Microglial calcium signaling is attenuated to neuronal activity in awake mice. *eLife*, 9. <https://doi.org/10.7554/eLife.56502>
- Umpierre, A. D., & Wu, L. J. (2020). How microglia sense and regulate neuronal activity. *Glia*, 69, 1637–1653. <https://doi.org/10.1002/glia.23961>
- Verderio, C., & Matteoli, M. (2001). ATP mediates calcium signaling between astrocytes and microglial cells: Modulation by IFN-gamma. *Journal of Immunology*, 166(10), 6383–6391.
- Vitrac, C., & Benoit-Marand, M. (2017). Monoaminergic modulation of motor cortex function. *Frontiers in Neural Circuits*, 11, 72. <https://doi.org/10.3389/fncir.2017.00072>
- Wendt, S., Maricos, M., Vana, N., Meyer, N., Guneykaya, D., Sementner, M., & Kettenmann, H. (2017). Changes in phagocytosis and potassium channel activity in microglia of 5xFAD mice indicate alterations in purinergic signaling in a mouse model of Alzheimer's disease. *Neurobiology of Aging*, 58, 41–53. <https://doi.org/10.1016/j.neurobiolaging.2017.05.027>
- Wolf, S. A., Boddeke, H. W., & Kettenmann, H. (2017). Microglia in physiology and disease. *Annual Review of Physiology*, 79, 619–643. <https://doi.org/10.1146/annurev-physiol-022516-034406>
- Zhang, Y., Chen, K., Sloan, S. A., Bennett, M. L., Scholze, A. R., O'Keefe, S., ... Wu, J. Q. (2014). An RNA-sequencing transcriptome and splicing database of glia, neurons, and vascular cells of the cerebral cortex. *The Journal of Neuroscience*, 34(36), 11929–11947. <https://doi.org/10.1523/JNEUROSCI.1860-14.2014>

SUPPORTING INFORMATION

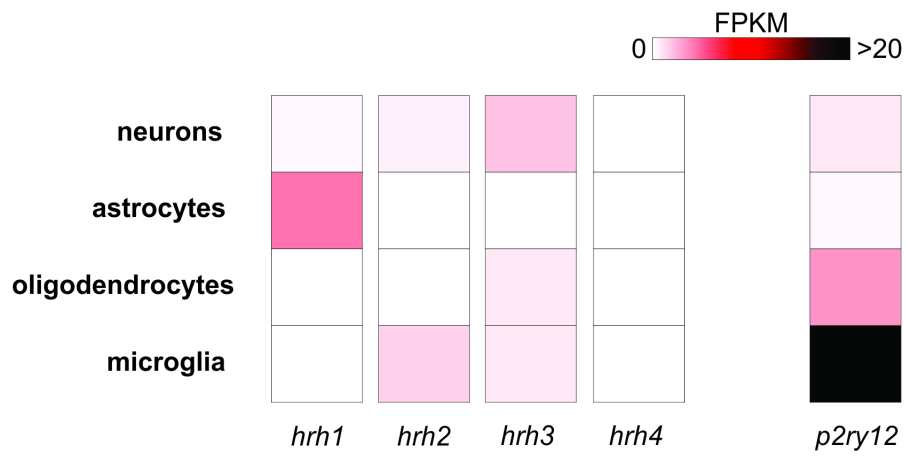
Additional supporting information may be found online in the Supporting Information section at the end of this article.

How to cite this article: Xia, P., Logiaco, F., Huang, Y., Kettenmann, H., & Sementner, M. (2021). Histamine triggers microglial responses indirectly via astrocytes and purinergic signaling. *Glia*, 1–14. <https://doi.org/10.1002/glia.24039>

Additional files

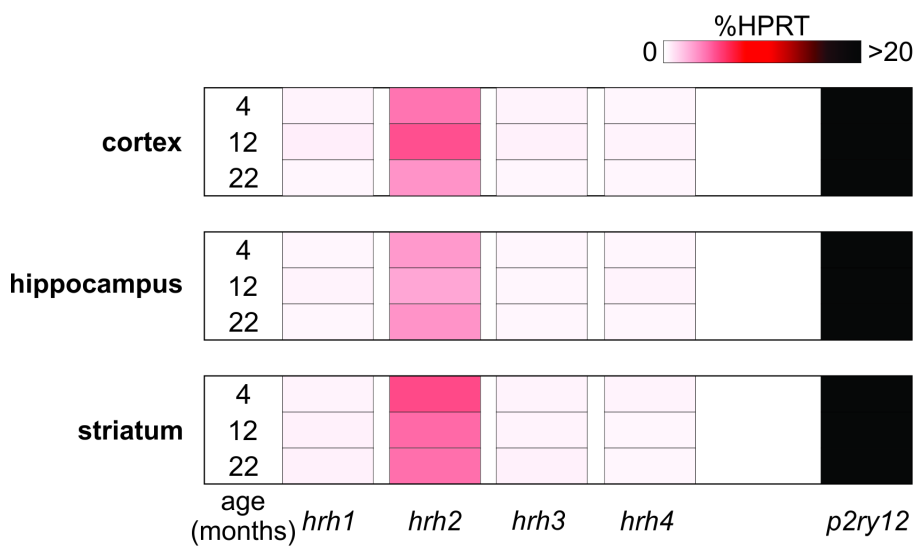
A

Zhang et al., 2014



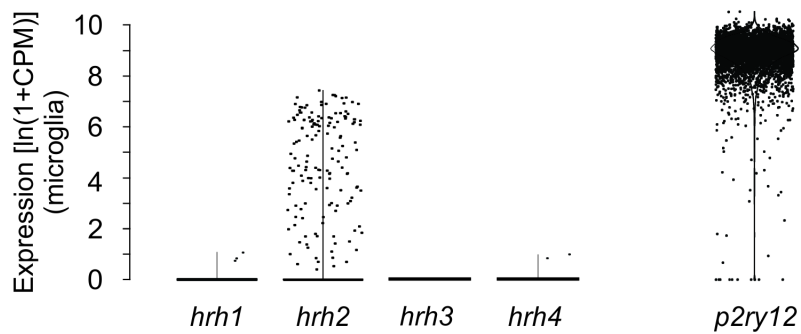
B

Grabert et al., 2016



C

Tabula Muris, 2018



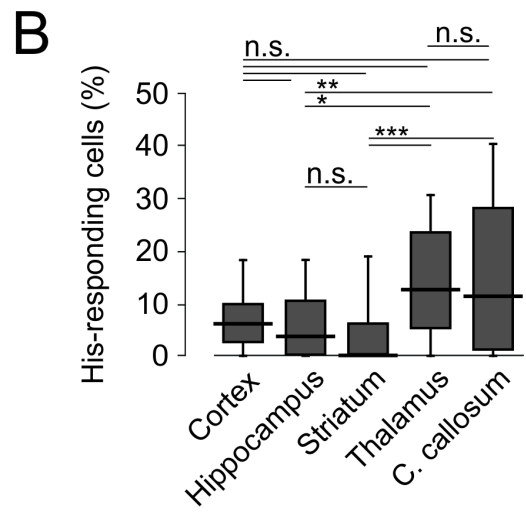
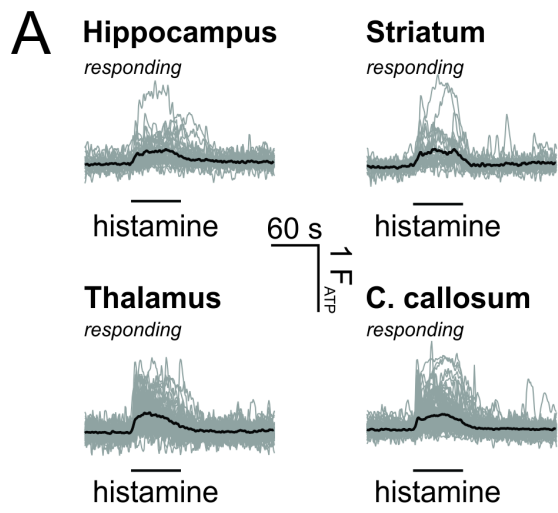
Suppl. Figure 1

Suppl. Figure 1. Microglial expression of histamine receptor isoforms - a meta-analysis

A. Metadata analysis from the bulk sequencing data set provided by Zhang *et al.* (2014). Neurons, astrocytes, oligodendrocytes (myelinating) and microglia were isolated by cell dissociation from whole mouse brain and subsequent FACS sorting using CD45 antibodies. Transcriptomics were assessed using an Illumina HiSeq 2000 Sequencer. Note that *Hrh1* is predominantly expressed in astrocytes; *Hrh2* in microglia and *Hrh3* in neurons, whereas there was no apparent expression of *Hrh4* in brain cells.

B. Metadata analysis from the bulk sequencing data sets provided by Grabert *et al.* (2016). Microglia were isolated by FACS sorting (CD11b, CD45, F4/80) of dissociated brain cells from different brain regions at different ages. Note that only *Hrh2* was detected in microglia from all investigated regions and ages.

C. Metadata analysis from data sets provided by the Tabula Muris consortium (2018). Single cell transcriptomic data were performed by mouse brain dissociation and subsequent FACS sorting for *CD11b*, *CD45* and *Tmem119* and by using a NovaSeq 6000 Sequencing System (Illumina). Note that *Hrh2* is the only histamine receptor isoform detected in microglial cells.



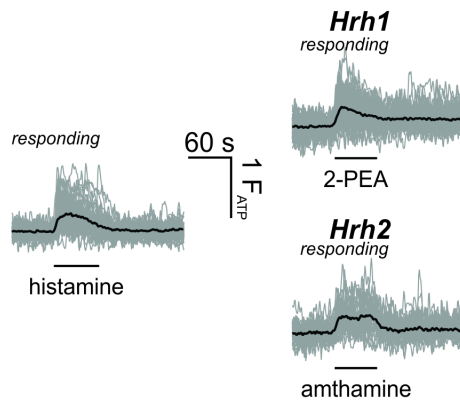
Suppl. Figure 2

Suppl. Figure 2. Histamine acts on microglia throughout the brain

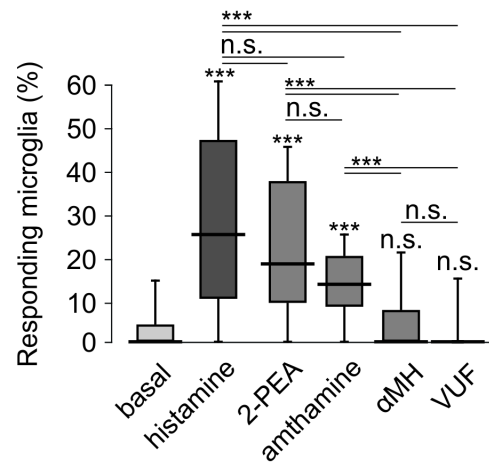
A. Overlay of intracellular Ca^{2+} responses from histamine-responding microglia in hippocampus, striatum, thalamus and corpus callosum. The black traces indicate the average response of all responding cells (gray).

B. Summary of the percentage of histamine-responding microglia in different brain regions. Data are presented as box plots which indicate the median (black line) as well as the 25-75% (box) and 10-90% (whiskers) percentiles. Statistical significance was tested by a Kruskal Wallis test followed by Dunn's multiple comparisons test and is indicated as followed: n.s., $p \geq 0.05$; *, $p \leq 0.05$; **, $p \leq 0.01$, ***, $p \leq 0.001$. Number of mice/slices/cells: N(Cortex) = 15/45/747; N(hippocampus) = 10/46/320; N(striatum) = 12/39/238; N(thalamus) = 13/47/613; N(corpus callosum) = 12/36/323.

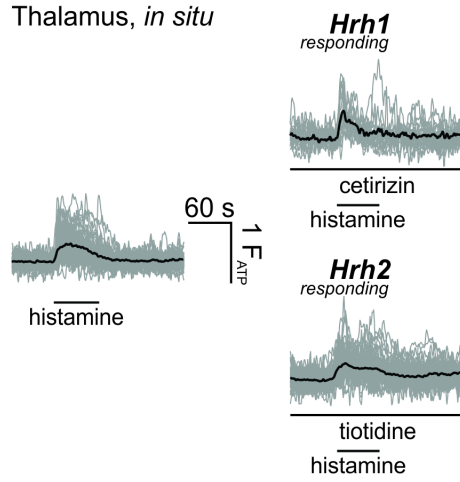
A Thalamus, *in situ*



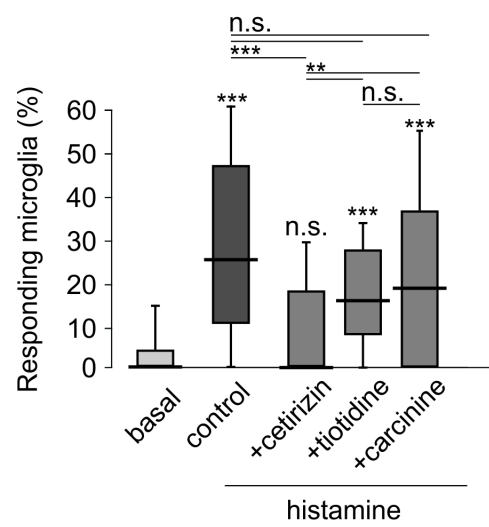
B



C Thalamus, *in situ*



D



Suppl. Figure 3

Suppl. Figure 3. Microglial histamine responses in thalamus originate from histamine receptors *Hrh1* and *Hrh2*

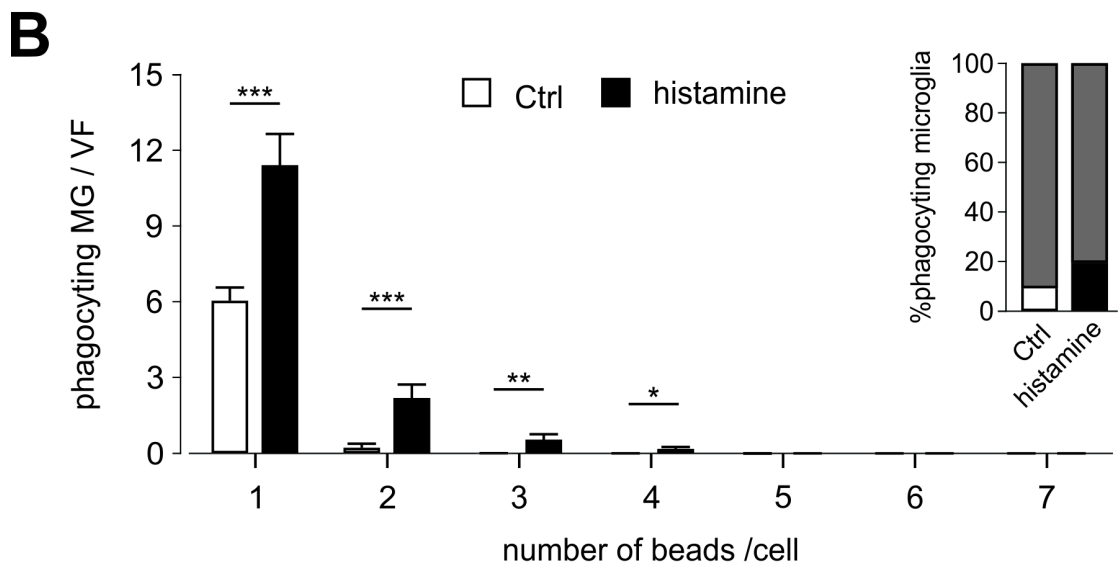
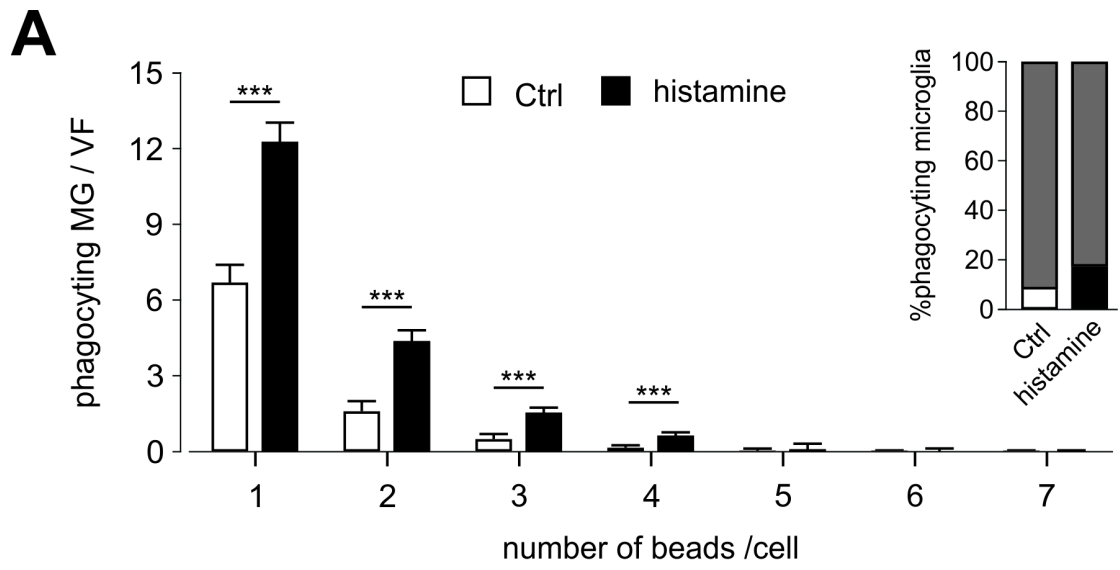
A. Overlay of intracellular Ca^{2+} responses from *in situ* thalamic microglia responding to histamine and the *Hrh1*- (2-PEA, 100 μM) and *Hrh2*- (Amthamine; 10 μM) specific agonists. Black traces indicate the average response of all responding cells (gray).

B. Summary of the percentage responding microglia from experiments shown in C, including those with *Hrh3*- (α -methylhistamine; 10 μM) and *Hrh4*- (VUF 10460; 10 μM) specific agonists.

C. Overlay of intracellular Ca^{2+} responses from thalamic microglia responding to histamine (100 μM) in the presence of subtype-specific *Hrh* receptor antagonists. Black traces indicate the average response of all responding cells (gray). Cetirizine (10 μM), tiotidine (10 μM) and carbinine (10 μM) are specific inhibitors of *Hrh1*, *Hrh2* and *Hrh3*, respectively.

D. Summary of the percentage responding microglia from experiments shown in A. Data are presented as mean \pm SEM. The following subtype-specific agonists were tested: *Hrh1*, cetirizine (10 μM); *Hrh2*, tiotidine (10 μM); *Hrh3*, carbinine (10 μM).

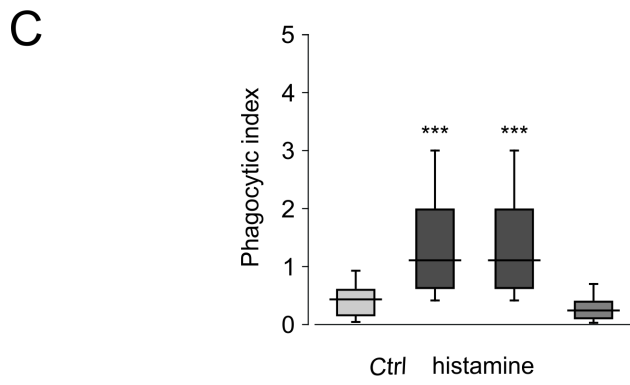
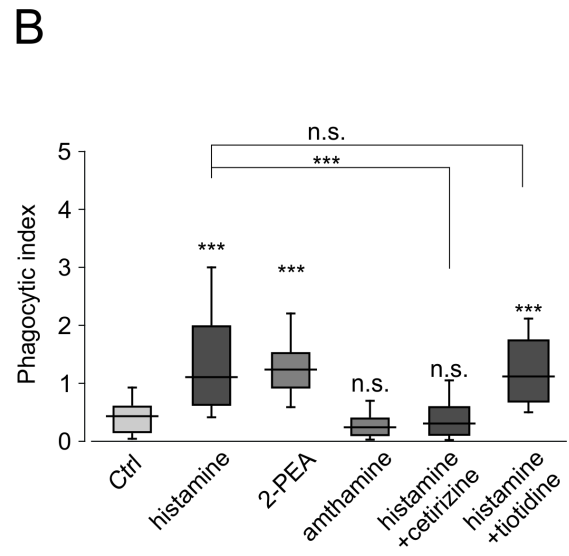
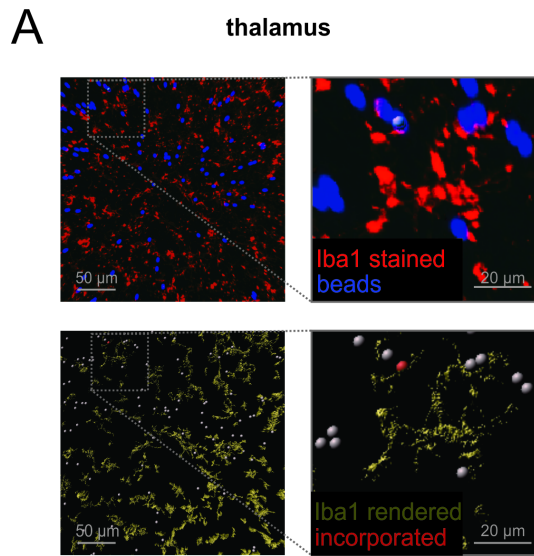
Data are presented as box plots which indicate the median (black line) as well as the 25-75% (box) and 10-90% (whiskers) percentiles. Statistical significance was tested by a Kruskal Wallis test followed by Dunn's multiple comparisons test and is indicated as followed: n.s., $p \geq 0.05$; *, $p \leq 0.05$; **, $p \leq 0.01$, ***, $p \leq 0.001$. Number of mice/slices/cells: N(basal) = 39/229/2250; N(histamine) = 13/47/613; N(2-PEA) = 6/43/396; N(amthamine) = 6/34/354; N(α MH) = 6/34/223; N(VUF) = 6/37/275; N(histamine+cetirizin) = 5/32/244; N(histamine+tiotidine) = 6/38/425; N(histamine+carbinine) = 6/40/358.



Suppl. Figure 4

Suppl. Figure 4. Stimulation of phagocytosis by histamine: estimation of the microglia number

Histogram showing the number of cortical (**A**) or thalamic (**B**) microglia per scanned view field with 1 or more incorporated beads. Control (white) and histamine (100 μ M; black) conditions are compared. *Inset* shows the percentage of phagocytosing microglia in relation to all microglia (i.e. including those without incorporated beads) at the two different conditions.



Suppl. Figure 5

Suppl. Figure 5. Microglial phagocytosis in the thalamus is stimulated by histamine via *Hrh1* and *P2ry12*

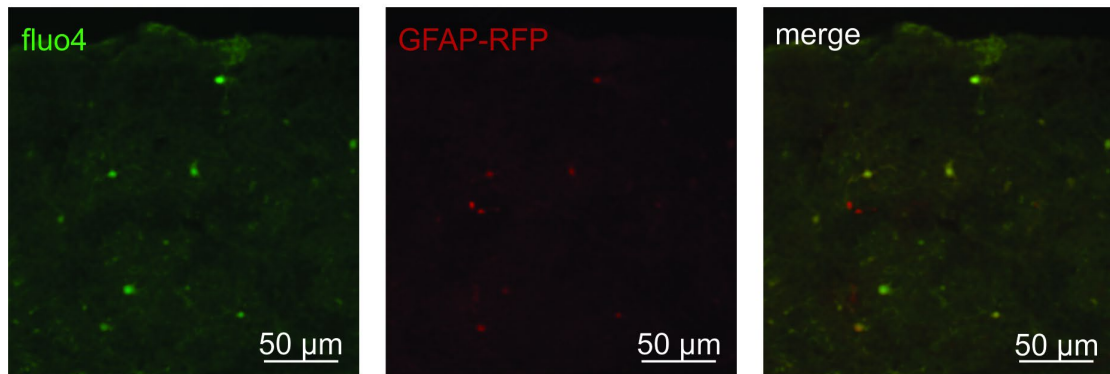
A. *Top*, Representative confocal image of Iba1-stained thalamic microglia (red) together with latex beads (blue) performed on brain slices from an adult WT male mouse. *Bottom*, 3D reconstruction of Iba1-positive microglia is shown with automatically counted phagocytosed beads (shown in red). Scale bars: 50/20 μm .

B. Comparison of phagocytic activity of cortical microglia under control conditions (white), in the presence of histamine (black), in the presence of the subtype-specific histamine receptor agonists 2-PEA (*Hrh1*; 100 μM gray) or amthamine (*Hrh2*; 10 μM ; gray) or in the presence of histamine plus the subtype-specific histamine receptor antagonists cetirizine (*Hrh1*; 10 μM ; black) or tiotidine (*Hrh2*; 10 μM ; black). Phagocytic index indicates the number of incorporated beads per Iba⁺ volume (see material and methods).

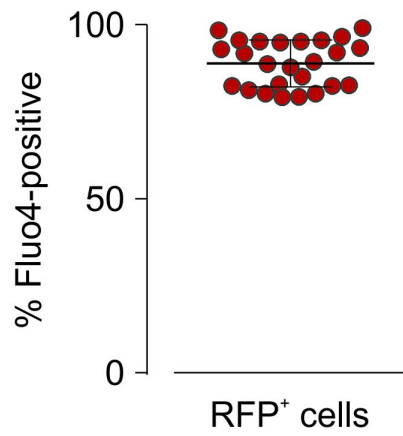
C. Effect of *P2ry12* blockade (1 μM AR-C69931) on microglial phagocytic activity under control and under histamine (100 μM)-stimulating conditions.

Data are presented as box plots which indicate the median (black line) as well as the 25-75% (box) and 10-90% (whiskers) percentiles. Statistical significance was tested by a Kruskal Wallis test followed by Dunn's multiple comparisons test and is indicated as followed: n.s., $p \geq 0.05$; *, $p \leq 0.05$; **, $p \leq 0.01$, ***, $p \leq 0.001$. Number of mice/slices: N(Ctrl) = 2/36; N(histamine) = 2/33; N(2-PEA) = 2/36; N(amthamine) = 2/36; N(histamine+cetirizin) = 3/34; N(histamine+tiotidine) = 2/36; N(ARC) = 2/36; N(histamine+ARC) = 2/36.

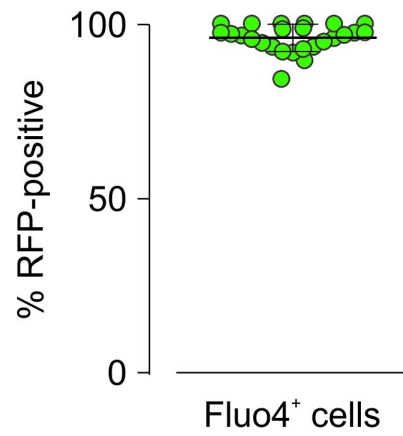
A



B



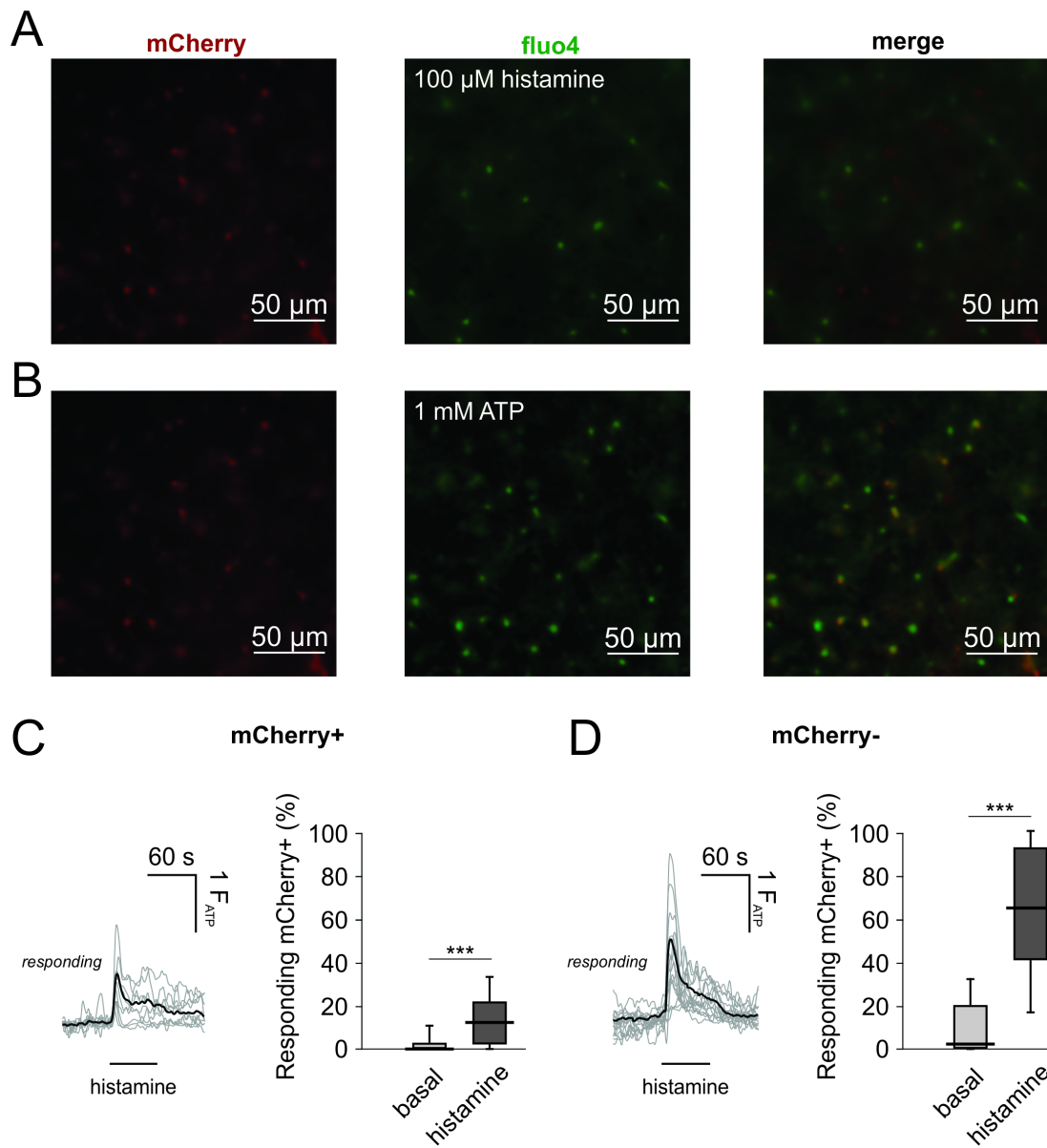
C



Suppl. Figure 6. Slice incubation with Fluo4 loads mainly GFAP+ cells.

A. Top, Representative confocal images of a Fluo4-labelled, cortical brain slice from a GFAP-RFP mouse at 488 nm (left) and 555 nm (middle) excitation wavelengths and the overlay of the two (right). Slices were incubated with 10 μ M Fluo4 for 30-40 min at 37°C and subsequently washed for 60-120 min in ACSF at room temperature. Note that only RFP+ cells took up Fluo4, and that there were only few RFP+ cells with no Fluo4 labelling. Scale bars: 50 μ m.

B and C. Quantification of the Fluo4 labeling of GFAP-RFP. The majority of GFAP+ cells were labelled with Fluo4 (**B**). Nearly all Fluo4-labelled cells were positive for GFAP (**C**). Each dot represents the percentage of GFAP+/Fluo4+ cells from one view field. We analyzed 25 view fields from 12 slices and 3 adult animals.



Suppl. Figure 7

Suppl. Figure 7. Cortical astrocytes and microglia respond differentially to histamine

A and B. Recording from an adult cortical brain slice of a Csf1R-2A-mCherry-2A-GCaMP6m mouse which was loaded and labelled with Fluo4. Left images (red) show microglia by their transgenic mCherry expression at the beginning of the experiment. Middle images are background-subtracted Fluo4/GCaMP6m signals evoked by 100 μ M histamine (**A**) or 1 mM ATP (**B**) Right images present an overlay of the mCherry and Fluo4/GCaMP6m channels. Note that mCherry+ cells only sparsely responded to histamine whereas most of the mCherry- cells displayed Ca²⁺ elevations (upper panels), consistent with the different response rates of microglia and astrocytes. Scale bar represents 50 μ m.

C and D. Traces on the right show the overlay of intracellular Ca²⁺ responses from cortical histamine-responding, mCherry+ (**C**) or mCherry- (**D**) cells. Black traces indicate the average response of all responding cells (gray). On the right, the percentage of histamine responding cells is summarized. Box plots indicate the median (black line) as well as the 25-75% (box) and 10-90% (whiskers) percentiles. Statistical significance was tested by a Kruskal Wallis test followed by Dunn's multiple comparisons test and is indicated as followed: n.s., $p \geq 0.05$; *, $p \leq 0.05$; **, $p \leq 0.01$; ***, $p \leq 0.001$. Number of mice/experiments/cells: N(Cx basal, mCherry+) = 4/12/160; N(Cx histamine, mCherry+) = 4/12/160; N(Cx basal, mCherry-) = 4/14/158; N(Cx histamine, mCherry-) = 4/14/158.

7. Curriculum Vitae

My curriculum vitae does not appear in the electronic version of my paper for reasons of data protection.

8. Publication List

1. Pengfei Xia, Francesca Loggiacco, Yimin Huang, Helmut Kettenmann, Marcus Semtner. Histamine triggers microglial responses indirectly via astrocytes and purinergic signaling. *Glia*. 2021 June 3. (Impact Factor: 5.984)
2. Huang Y, Zhang Q, Lubas M, Yuan Y, Yalcin F, Efe I, Xia P, Motta E, Buonfiglioli A, Lehnardt S, Dzaye O, Flueh C, Synowitz M, Hu F, Kettenmann H. "Synergistic Toll-like receptor 3/9 signaling affects properties and impairs glioma-promoting activity of microglia." *The Journal of Neuroscience*. 2020 July 6. (Impact Factor: 5.673)
3. Huang Y, Zhang B, Haneke H, Haage V, Lubas M, Yuan Y, Xia P, Motta E, Nanvuma C, Dzaye O, Hu F, Kettenmann H. "Glial cell line-derived neurotrophic factor increases matrix metalloproteinase 9 and 14 expression in microglia and promotes microglia-mediated glioma progression." *Journal of Neuroscience Research*. 2021 Jan 6. (Impact Factor: 4.699)

9. Acknowledgements

Now writing to this chapter, I would like to take this opportunity to thank to all those persons that have given their invaluable support and assistance.

First, I would like to express deep gratitude to Prof. Dr. Helmut Kettenmann for giving me the opportunity to study and work in their lab and let me pursue my Dr. med. In the nearly three years of working with you, encouraged me and provided great idea of the project. Also, I would like to thank to Dr. Marcus Semtner who supervised and enlightened me how to make better science work, you always supported me with your continuous patience and fruitful discussions.

In addition, I also thank to Yimin Huang, Francesca Logiacco, Nirmeen Elmadany and Svilen Georgiev for the scientific discussions and infinite support which really encouraged me to continue my project. Special thanks to Birgit Jarchow, you are always very enthusiastic to help me solve all kinds of difficulties inside and outside the lab, your positive attitude towards life can always give me great encouragement. I am very thankful to Regina Piske, Nadine Scharek and Maren Wendt for the great technical supports. Moreover, I would like to thank all members of the Kettenmann lab, for all the happy and sad moments we worked together.

Besides, I want to thank my friends Pu Huang, Qing Li, Shixian Yan, Cheng Zhong and Shuai Zhu for all the laughs we had together.

Finally, I would like to thank my family for your continuous supporting and encouraging me, shaping me to the person that I am.

Thank you all
Pengfei